Maintaining Cardiac and Gastric Physiology:

TRIM Proteins as Central Factors in Regulation of Organ Homeostasis at the Cellular Level

Dissertation

Presented in Partial Fulfillment of the Requirements for the Degree Doctor of Philosophy in the Graduate School of The Ohio State University

By

Kristyn Nicole Gumpper

Biomedical Sciences Graduate Program

The Ohio State University

2019

Dissertation Committee

Jianjie Ma, PhD, Advisor

Peter Mohler, PhD

Jackie Wood, PhD

Jian-Qiu Wu, PhD

Renzhi Han, PhD

Abstract

Maintaining cellular homeostasis is an essential aspect of maintaining physical health and dysregulation of cellular homeostasis leads to potentially life-threatening pathological disorders. For example, coronary heart disease, or heart attacks, affects approximately 635,000 Americans a year and about 300,000 with a recurrent attack with high morbidity and mortality rates. While diseases like Gastro-Esophageal Reflux Disorder, although not necessarily life-threatening, still require a lifetime of antacid medications. Living organisms have developed intrinsic mechanisms to maintain and counteract disruptions in homeostasis. In order to improve outcomes for patients and develop new therapies for diseases like heart attacks and GERD, we must better understand the mechanisms behind how homeostasis is maintained or reestablished. Recently, TRIM family proteins have been identified as essential factors that mediate protein catabolism, as well as other functions in cell-associated innate immunity, cancer, membrane repair, and autophagy, to name a few. Of interest are TRIM72, also known as MG53, and TRIM50. MG53 is essential to cell plasma membrane repair after mechanical or chemical injury, making it an attractive therapeutic agent to treat cardiovascular diseases. Additionally, MG53 may have a novel function in mitochondria protection. TRIM50 has recently been described as a regulator of gastric acid secretion in parietal cells. These two proteins share a common N-terminal TRIM domain; however, they have divergent PRY/SPRY domains. Given the

prevalence of the PRY/SPRY domain encoded in the human genome and within the TRIM family and the apparent importance of MG53 and TRIM 50, the goal of this this dissertation research was to elucidate the roles of MG53 in mitochondrial protection and TRIM50 in gastric acid secretion. I hypothesize the divergent functions are driven by the divergent C-terminal PRY/SPRY domains. Through confocal imaging and biochemical analysis, I show MG53 does localize to mitochondria after oxidative injuries and this localization prevents mitochondrial damage. In a TRIM50 knockout mouse model, I show TRIM50 is essential for maintaining the cell's ability to buffer its internal contents which, in turn, causes a dysregulation of gastric acid secretion upon stimulation. Finally, generating chimeric proteins between the N-terminal and C-terminal domains of MG53 and TRIM50, I show the divergent C-terminal domain of MG53 connected to the conserved N-terminal domain of TRIM50 is insufficient for providing the well-established membrane repair function of MG53. Overall, this dissertation provides evidence of a novel function of MG53 in maintaining cellular homeostasis through mitochondrial protection. Identifying this novel function brings us one step closer to being able to make MG53 a therapeutic approach after oxidative injuries such as coronary heart disease. Additionally, the results I present in this dissertation suggests a new mechanism for TRIM50's involvement in gastric acid secretion. Finally, this dissertation clarifies role of the MG53 PRY/SPRY domain in membrane repair.

Dedication

To my parents

For believing in your “absent minded professor”

and

To Andy Fedus

My support, my sanity, and my IT guy

Acknowledgments

I would like to thank all the members of the Ma lab for their assistance and comments on my research projects during my Ph.D. In particular, I would like to thank Dr. Pei-Hui Lin for her constant support, scientifically and personally, throughout my 6 years in the laboratory of Dr. Jianjie Ma. I would also like to thank Dr. Ki Ho Park his assistance in performing myocardial infarctions, collecting cardiomyocytes and using the lab microscopes. I would like to thank Dr. Jianjie Ma for his support and patience as I worked through the development of assays essential to my projects. Thank you for having me in your lab and pushing me to grow as a scientist.

In addition to the Ma Lab, I would like to thank my Dissertation Committee. I appreciate all their advice and support throughout the years as I developed these projects. A large thank you to Dr. Renzhi Han and Dr. Jingsong Zhou for their support in providing references for me for the American Heart Association Fellowship application. Finally, I would like to thank the American Heart Association for their financial support in awarding me a Pre-Doctoral Fellowship for 2018-2019.

Vita

Experience

Adjunct Faculty 2019 – Present
Columbus State Community College, Columbus, OH
Course: Human Physiology

M.S. Thomas Jefferson University, Microbiology & Immunology May 2012

Lab Specialist 2011 – 2012
Thomas Jefferson University, Philadelphia, PA
PI: Masumi Eto, PhD

B.S. Allegheny College, Biology May 2010
Minor in Music Performance (Vocal)

Publications

1. Khasnis M, Nakatomi A, **Gumpper K**, Eto M (2014) Reconstituted human myosin light chain phosphatase reveals distinct roles of two inhibitory phosphorylation sites of the regulatory subunit, MYPT1. Biochemistry. doi: 10.1021/bi5001728

2. Park KH, Weisleder N, Zhou J, **Gumpper K**, Zhou X, Duann P, Ma J, Lin P-H (2014) Assessment of calcium sparks in intact skeletal muscle fibers. J Vis Exp. doi: 10.3791/50898

3. Sun M, Huang J, Bunyak F, **Gumpper K**, De G, Sermersheim M, Liu G, Lin P-H, Palaniappan K, Ma J (2014) Superresolution microscope image reconstruction by spatiotemporal object decomposition and association: Application in resolving t-tubule structure in skeletal muscle. Opt Express. doi: 10.1364/OE.22.012160

4. Huang J, **Gumpper K**, Chi Y, Sun M, Ma J (2015) Fast two-dimensional super-resolution image reconstruction algorithm for ultra-high emitter density. Opt Lett. doi: 10.1364/OL.40.002989

5. Huang J, Sun M, **Gumpper K**, Chi Y, Ma J (2015) 3D multifocus astigmatism and compressed sensing (3D MACS) based superresolution reconstruction. Biomed Opt Express. doi: 10.1364/BOE.6.000902

6. Lin, P-H, Duann P, Komazaki S, et al (2015) Lysosomal two-pore channel subtype 2 (TPC2) regulates skeletal muscle autophagic signaling. J Biol Chem. doi: 10.1074/jbc.M114.608471

7. Lin, P-H, Sermersheim M, Li H, Lee PHU, Steinberg SM, Ma J (2017) Zinc in Wound Healing Modulation. Nutrients. doi: 10.3390/nu10010016

8. Sermersheim MA, Park KH, **Gumpper K**, Adesanya TMA, Song K, Tan T, Ren X, Yang J-M, Zhu H (2017) MicroRNA regulation of autophagy in cardiovascular disease. Front. Biosci. - Landmark 22:

9. Wang S*, **Gumpper K***, Tan T, et al (2018) A novel organ preservation solution with efficient clearance of red blood cells improves kidney transplantation in a canine model. Cell Biosci 8:28

10. Ayodele Adesanya TM, Russell M, Park KH, et al (2019) MG53 protein protects aortic valve interstitial cells from membrane injury and Fibrocalcific Remodeling. J Am Heart Assoc. doi: 10.1161/JAHA.118.009960

11. **Gumpper K**, Sermersheim M, Zhu MX, Lin P-H (2019) Skeletal muscle lysosomal function via cathepsin activity measurement. Methods Mol Biol. doi: 10.1007/7651_2017_64

12. **Gumpper K**, Ma J (2019) Zinc Signaling in Skeletal Muscle. Zinc Signals Cell. Funct. Disord. *In Press*

13. Bian Z, Wang Q, Zhou X, et al (2019) Sustained Elevation of MG53 in the Bloodstream Increases Tissue Regenerative Capacity without Compromising Metabolic Function. Nat Commun *In Press*

Fields of Study

Major Field: Biomedical Sciences Graduate Program
Graduate Interdisciplinary Specialization in College and University Teaching

Table of Contents

List of Tables

List of Figures

Chapter 1. Introduction

Physiology is the study of "normal" functions of living organisms and how those organisms maintain homeostasis, or equilibrium. Organisms use a variety of methods to maintain homeostasis such as modulating ion transport, protein synthesis, and protein degradation. When one or more of these methods is interrupted or altered, homeostasis is lost, causing pathologies like inflammation, disease susceptibility, and necrosis, to name a few. As life became more complex cells and organisms evolved many elegant mechanisms to maintain homeostasis. Many of these mechanisms involve regulating ion concentrations across membranes for functions like energy production as well as intra- and extra-cellular signaling. Other mechanisms rely on the regulation of protein biogenesis, localization, or catabolism.

In 2004, the regulation of homeostasis through catabolism via a ubiquitin-mediated pathway won Aaron Ciechanover, Avram Hershko and Irwin Rose the Nobel Prize in Chemistry [1]. In this pathway, E1 activating enzymes provide energy to ubiquitin or ubiquitin- like proteins including Nedd8 and small ubiquitin modifier (SUMO) by using ATP to create a thioester bond between ubiquitin and itself, releasing AMP. The energized E1 and ubiquitin complex binds with the catabolic E2 enzyme to transfer the thioester bond from the E1 enzyme to the E2 enzyme, releasing the E1 enzyme [2]. When an E3 ubiquitin ligase enzyme encounters its substrate, it will form a

complex with the substrate protein and the E2/ubiquitin complex. From there, the E3 ligase facilitates ubiquitin transfer from the E2 enzyme to specific lysines on the substrate protein. After mono- or poly-ubiquitination, the tagged substrate protein will be transported to the proteasome where it gets degraded into amino acids and small peptide chains and ubiquitin will be released for future use. Therefore, E3 ubiquitin ligases act as regulators of protein and organelle catabolism, or degradation, and are historically categorized into two groups: RING (really interesting new gene) type and HECT (homologous to the E6AP carboxyl terminus) type E3s [3]. **In order to understand some ways cells have evolved to maintain cellular and tissue homeostasis through mechanisms like ubiquitination, we must understand the diverse roles of TRIM family proteins.**

TRIM family proteins: Diversity in form and function

TRIM proteins have been implicated in a variety of cell and tissue processes including but not limited to differentiation, development, autophagy, immunity, and oncogenesis [4–7]. Over 75 TRIM proteins coded for in the human genome with some of these proteins be conserves across vertebrate and invertebrate species [8]. They are all zinc binding proteins containing a conserved amine (N) terminal domain, also known as the RBCC or TRIM domain, consisting of a RING domain, one or two B-box domains, and a Coiled-coil domain. TRIM family proteins are further subclassified into eleven subfamilies by their divergent carboxy (C) terminal domains, as seen in Table 1 [4, 5]. Most known TRIM protein functions arise from the conserved RBCC domain as a zinc binding E3 ubiquitin ligase domain.

Table 1 TRIM Subfamilies

Subfamily	TRIM Domain	C-Terminal Domain	Subfamily Members
C-I	R-B1-B2-CC-	-COS-FN3-PRY-SPRY	MID1, MID2, TRIM9, TIRM46, TRIM67
C-II	R---B2-CC-	-COS-----	TRIM54, TRIM55, TRIM63
C-III	R-B1-B2-CC-	-COS-FN3---	TRIM42
C-IV	R-B1-B2-CC-	----PRY-SPRY	TRIML1, TRIM4, TRIM5a, TRIM7, TRIM10, TRIM11, TRIM15, TRIM17, TRIM21, TRIM22, TRIM25, TRIM26, TRIM27, TRIM34, TRIM35, TRIM38, TRIM39, TRIM41, TRIM43, TRIM47, TRIM48, TRIM49, TRIM50, TRIM53, TRIM58, TRIM60, TRIM62, TRIM69, TRIM72, TRIM75
C-V	R-B1-B2-CC-	------	PML, TRIM8, TRIM31, TRIM40, TRIM52, TRIM61, TRIM73, TRIM74
C-VI	R-B1-B2-CC-	-PHD-BROMO----	TRIM24, TRIM28, TRIM33
C-VII	R-B1-B2-CC-	-FIL-NHL----	TRIM2, TRIM3, TIRM32, TRIM71
C-VIII	R---B2-CC-	-MATH----	TRIM37
C-IX	R-B1-B2-CC-	-ARF----	TRIM23
C-X	R-B1-B2-CC	-FIL-----	TRIM45
C-XI	R---B2-CC-	-TM----	TRIM13, TRIM59

Adapted from Ozato, K et al. 2008 [4] *and Hatakeyama 2011* [5]

Within this family of proteins, the divergent C-terminal domains provide functional and subcellular localization specificity. TRIM proteins with the PHD-BROMO domains often function as transcriptional co-activators or co-repressors often associated with oncogenes [6, 9]. Indeed, investigations into the role of the PHD and BROMO domains showed both domains together were necessary for interreacting with the nucleosome [10]. Interestingly, the nuclear transcriptional function of TRIMs 24, 28 and 33 are not associated with their functional ubiquitin ligase domain, the RING domain,

rather, it is directly associated with their c-terminal domain [9, 11]. However, TRIM33 is also known to ubiquitinate Smad4 for degradation, exhibiting unique multi-function properties seen in some TRIM proteins, regardless of c-terminal domain characteristics [6].

Subfamily C-II containing a c-terminal subgroup one signature (COS) domain. Sub-group C-II proteins TRIMs 63, 55, and 54 are also known as Muscle RING Fingers, or MuRF-1, -2, or -3, respectively [12, 13]. These TRIM proteins are essential for maintaining skeletal muscle homeostasis through direct interactions with myofibrillar proteins like titin, nebulin, troponin-I, troponin-T, and myosin light chain 2, to name a few [12]. Deletions or mutations in these proteins often lead to multiple functional and metabolic disorders in skeletal muscle like cachexia and sarcopenia [13–15].

The c-terminal PRY/SPRY, or B30.2, domain characterizes the largest subfamily of TRIM proteins with, arguably, the most diverse functions [4, 6, 16]. The PRY/SPRY domain has an antibody-like structure with four variable loops in the gene sequence and is found in over 500 identified human proteins in the SMART database [16, 17]. This variable loop allows for diverse protein-protein interactions, even within the same family of proteins like TRIM proteins. Indeed, this subfamily of TRIM proteins is dynamic, evolving much faster than other TRIM subfamily types [8]. For example, PRY/SPRY containing TRIMs 1, 5α, 19, 22 and 32 participate in innate immunity, recognizing motifs within retroviral capsid proteins and ubiquitinating them for proteasomal degradation [16, 18]. PRY/SPRY containing TRIMs 9, 27, and 33 translocate to loci of oncogenes in various cancers with TRIMs 11, 25, 26, 62, and 72 either positively or negatively

regulating TGF-β signaling [6, 19, 20]. Interestingly, for some TRIM proteins, like PRY/SPRY containing TRIM72 and TRIM50, their non-ubiquitination related functions are better characterized. **Understanding the non-ligase functions of TRIM proteins like TRIM72 and TRIM50 will move towards a better understanding of functions of the PRY/SPRY domain**.

Membrane Repair for Tissue Protection and Regeneration

Cell membrane damage is caused by many types of physical or chemical perturbations to the lipid bilayer; whether that is a physical cut, locomotion-induced tearing, or contact with pore forming toxins, to name a few. When a hole is formed in the plasma membrane, ions within the cell (K^+ and Cl^-) rush out of the cell, down their concentration gradient, while ions outside the cell (Ca^{2+}, Na^+, and Mg^{2+}) rush in. Most importantly, the inrush of Ca^{2+} into the cell causes a dramatic increase in intracellular Ca^{2+}, which is one of the major intracellular signaling molecules whose persistence inside the cell at a high concentration will activate autophagy or apoptosis [21, 22]. Because Ca^{2+} is integral to most signaling pathways within the cell, Ca^{2+} concentration is highly buffered [23, 24]. Theoretically, this means the influx of extracellular Ca^{2+} only affects the organelles like the ER and lysosomes immediately surrounding breaks in the plasma membrane. Too large a wound in the plasma membrane, therefore, would cause aberrant Ca^{2+} signaling, leading to cell death. Because of this, living organisms have developed several mechanisms for repairing holes in the plasma membrane: contraction, exocytosis, patching, internalization, externalization, and plugging [22].

Plasma membrane contraction involves recruitment and formation of an actomyosin ring around the injury site. From there, the hole in the membrane seals following a mechanism similar to membrane sealing for cytokinesis. Internalization and externalization, and exocytosis are mechanisms proposed for sealing small holes in the membrane. For exocytosis, the increase in intracellular calcium signals for movement of vesicles to the plasma membrane to effectively add additional lipid bilayer to force the hole closed. In internalization, an invagination would form at the region of membrane with the hole that would be pinched off, similarly to receptor-mediated endocytosis. Opposite of internalization is externalization where plasma membrane around the hole is externalized via ESCRT-mediated budding [22, 24]. Plugging and patching can both filler larger gaps in the plasma membrane with the recruitment of intracellular vesicles, however patching only stoppers holes without re-establishing a continuous membrane [25]. Whereas, patching occurs as the influx of extracellular calcium signals to TRPML1 transiently release lysosomal Ca^{2+}, activating Ca^{2+} sensors like synaptotagmins, ferlins, and annexins to fuse lysosomal vesicles for exocytosis-like repair [24, 26]. **These mechanisms are still not fully defined and require more study to better understand the various ways our cells re-establish homeostasis through membrane resealing.**

TRIM72/MG53: Regenerative Medicine's "Miracle Protein"

In 2009, Cai et al. described a novel TRIM protein TRIM72, at the time named MG53, while elucidating what proteins are involved in maintaining the structure of the skeletal muscle t-tubule and calcium signaling. Unlike any other PRY/SPRY containing TRIM protein, MG53 mediated patch or exocytosis-associated plasma membrane repair.

A coordinated event by oxidative sensor MG53 and Ca^{2+} sensor annexin V bind to the exposed membrane lipid phosphatidylserine (PS) while interacting with caveolin 3 and dysferlin to form a membrane repair "patch" [27–29]. Without MG53, dysferlin-associated vesicles cannot migrate to the injured plasma membrane, resulting in a significant reduction of cell survival [28].

The repair function depends on MG53 ability to polymerize upon changes in oxidative state. For this, cysteine 242 located between the coiled-coil and PRY domains, but not cystine 313 in the middle of the PRY domain is responsible for polymerization. Mutations in cysteine 242 result in an inability to polymerize, as shown in western blotting experiments with or without DTT as an oxidative reducer [27]. This inability to polymerize was directly correlated with a significant reduction in nucleation at the plasma membrane injury site and increased entry of FM4-64 dye into wounded cells [27]. In addition to polymerization for membrane repair, MG53 requires cholesterol-associated lipids for translocation to damaged plasma membrane as well as the molecular motor non-muscle myosin IIA [30, 31]. Other RBCC motifs have been identified as essential for its membrane repair function of MG53 such as the two leucine zippers found in the coiled-coil domain [32] and the two zinc-finger in the RING and B-box domains [33]. MG53 is incapable of migrating to the plasma membrane without the ability to bind to zinc or if zinc is chelated, as indicated in Figure 1 [33, 34]. Altogether, these components of MG53 allow interaction with lipid rafts and vesicles inside the cell and nucleate at a damaged plasma membrane for repair and cell survival.

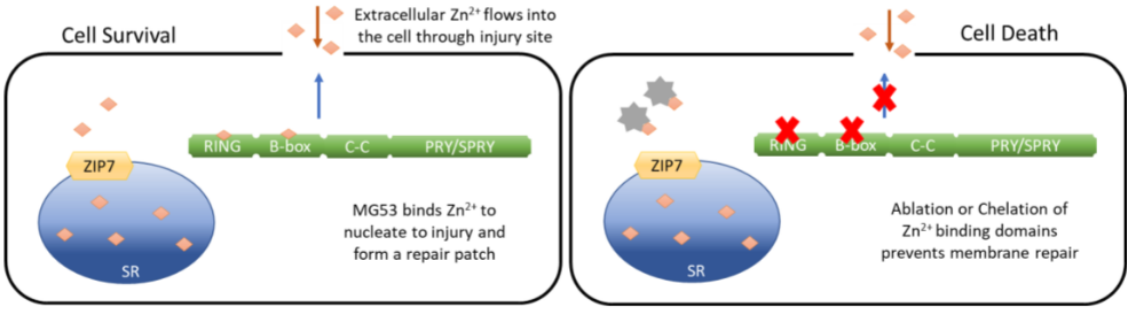

Figure 1 MG53 binds zinc for membrane repair.

Zinc binding to the RING and B-Box of MG53 contributes to repair of injury to skeletal muscle through facilitation of intracellular vesicle trafficking to the injury site.

See ref 34 (Gumpper and Ma, book chapter)

As an essential mediator of plasma membrane repair, many studies have assessed MG53's ability to prevent or heal various injuries such as membrane fragility in Duchenne's Muscular Dystrophy [35–37], dermal wounds [20], calcification of aortic valvular interstitial cells [38], and ischemic damage to multiple tissue types including, but not limited to: skeletal muscle, lung, kidney, and brain [28, 29, 39–44]. Indeed, one of the best characterized functions of MG53's tissue protection is in response to ischemia / reperfusion (I/R) injury which causes oxidative damage to cells. MG53 has been implicated in regulating the PI3K/Akt/mTOR pathway during oxidative stress injuries by inducing phosphorylation of Akt, glycogen synthase kinase-3β (GSK-3β), and ERK1/2 [45]. Additionally, MG53's protection of cell membrane integrity can reverse muscle degeneration in several muscular dystrophy models via activation of the cell survival Akt, ERK1/2, and GSK-3β pathway [29, 35, 46].

As an E3 ubiquitin ligase, MG53 has two known substrates, IRS-1 and focal adhesion kinase (FAK), for regulation of cell differentiation and proliferation [47]. During myogenesis, total FAK is transiently reduced by MG53 via ubiquitination, a critical step after cell commitment to differentiation. After the temporary reduction in FAK, expression is increased to promote fusion of myoblasts into myotubes [48].

Since its initial discovery in 2009, many groups have worked towards understanding MG53 in physiology and how to target MG53 for tissue repair in regenerative medicine. As it turns out, MG53 may be a mediator in metabolic syndrome and insulin signaling in skeletal muscles, however this function is hotly debated [33, 49, 50]. Song et al. reported MG53 expression was markedly elevated in animal models of insulin resistance, related to MG53's ubiquitination of IRS-1 [51]. Adverse effects of MG53 as an E3 ligase in harnessing IRS1-mediated insulin signaling and metabolic function in muscle have been reported [50, 52–54]. Additionally, they suggest muscle samples derived from the db/db mice and human patients exhibit elevated MG53, however this has not been reproducible in some studies on MG53 [49, 52]. Additionally, there are three other homologous proteins in the IRS family all of which contribute to insulin signal transduction in skeletal muscle. An absence of IRS-1 or IRS-3 is not enough to induce type II diabetes [55, 56]. Only through a combination of IRS-1 and IRS-3 deficiency does a manifestation of diabetic phenotypes result, indicating that IRS-1 and IRS-3 serve overlapping physiological functions in insulin signaling[56]. Thus, MG53-mediated IRS-1 down-regulation cannot solely induce type II diabetes. Indeed, we show MG53 expression remains unchanged in skeletal muscle after a high fat diet that

resulted in metabolic syndrome, and less MG53 is secreted into the blood stream [49, 50]. Additional toxicological studies on MG53 in both mice and beagle dogs indicate that repeated i.v. administration of MG53 results in no adverse effects with no changes to blood glucose or other pathological changes [29, 40].

The above-mentioned studies on MG53 included many imaging experiments analyzing the movement and subcellular localization of MG53 that was either fluorescently tagged via plasmid or conjugation to an NHS-ester dye. Although plasma membrane repair is an incredibly important mechanism for cell survival, many imaging studies also revealed a scattering of MG53 throughout the cytoplasm of the cell that has not been well understood. As seen in Figure 2, after high-fat diet induced oxidative stress, MG53 localized to both the sarcolemma membrane and to COX-IV a commonly used marker for mitochondria [49]. **This novel MG53 localization around the mitochondria**

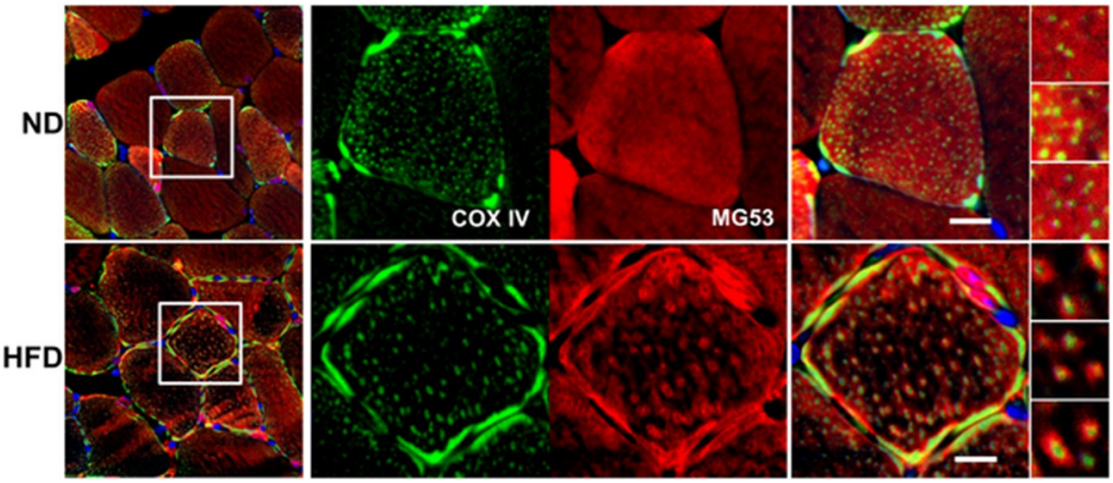

Figure 2 MG53 Surrounds COX IV After Oxidative Stress

Skeletal muscle from mice fed a long term normal or high fat diet stained for mitochondrial marker COX IV (green) and MG53 (red)

Adapted from Ma et al. [49]

suggests MG53 may be aiding cell survival through the maintenance of mitochondria integrity via mitophagy.

Mitophagy and Reactive Oxygen Species: Driving Diseases

The concept of ROS accumulation was established over 50 years ago by Denham Harman whose theory asserted that aged cells accumulate free radicals [57, 58]. This accumulation of ROS as we age is associated with many diseases like diabetes, cancer, neurodegenerative disorders, and ischemia-reperfusion injuries, to name a few. To combat an accumulation of ROS inside the mitochondria, cells express three different superoxide dismutases (SODs) that bind metals like zinc and copper, manganese or iron to transform superoxides into H_2O_2 and O_2. Mutations in these proteins have been associated with degenerative diseases such as mutations in Cu-Zn-SOD1 contributing to the ROS buildup seen in neurons in amyotrophic lateral sclerosis (ALS). Mn-SOD2 is found primarily in mitochondria and loss of activity for this protein contributes to the progression of Alzheimer's and Parkinson's disease [59]. Sometimes, ROS accumulation in mitochondria cannot be overcome by SOD function, leading to mitochondrial damage. To preserve cellular function, damaged mitochondria must be removed from the cell in a highly regulated process, maintaining a healthy pool of mitochondria in a process called mitophagy.

Autophagy is a highly regulated process whereby the cell removes unwanted or damaged organelles or other cellular components. Mitophagy is the specific autophagic process where damaged mitochondria are degraded for recycling into other cellular

components. As seen in Figure 3, when mitochondria are damaged, ATP production is reduced with a concurrent secretion of the mitochondrial-specific reactive oxygen species (ROS) O_2^- as well as mitochondrial proteins like cytochrome c through the mitochondrial permeability transition pore [60, 61]. If the damaged mitochondria secreting ROS are not removed, a negative feedback loop known as "ROS-induced ROS-release" will occur, damaging more mitochondria leading to cell death [60, 61].

In normal cells or under limited stress, the damaged mitochondria are partitioned from healthy mitochondria via Drp1-associated fission [62]. From there, E3 ubiquitin ligases like PINK1 and Parkin nucleate at the damaged mitochondria to ubiquitinate proteins on the outer mitochondria membrane that are exposed after damage [63–65]. An autophagosome forms around the ubiquitinated mitochondria in an Atg8, p62, LC-3 dependent manner. The formed autophagosome merges with a lysosome for degradation of the damaged mitochondria to recycle building blocks for future use. Although the PINK1/Parkin mechanism is the best understood, there are other E3 ubiquitin ligases responsible for tagging damaged mitochondria. Recent studies have indicated metabolically demanding tissues like brain and heart exhibit PINK1-independent mitophagy that is not well defined [66, 67]. **It is imperative we explore the possible function of MG53 in mitochondrial maintenance or mitophagy as we move towards making MG53 into a therapeutic agent.**

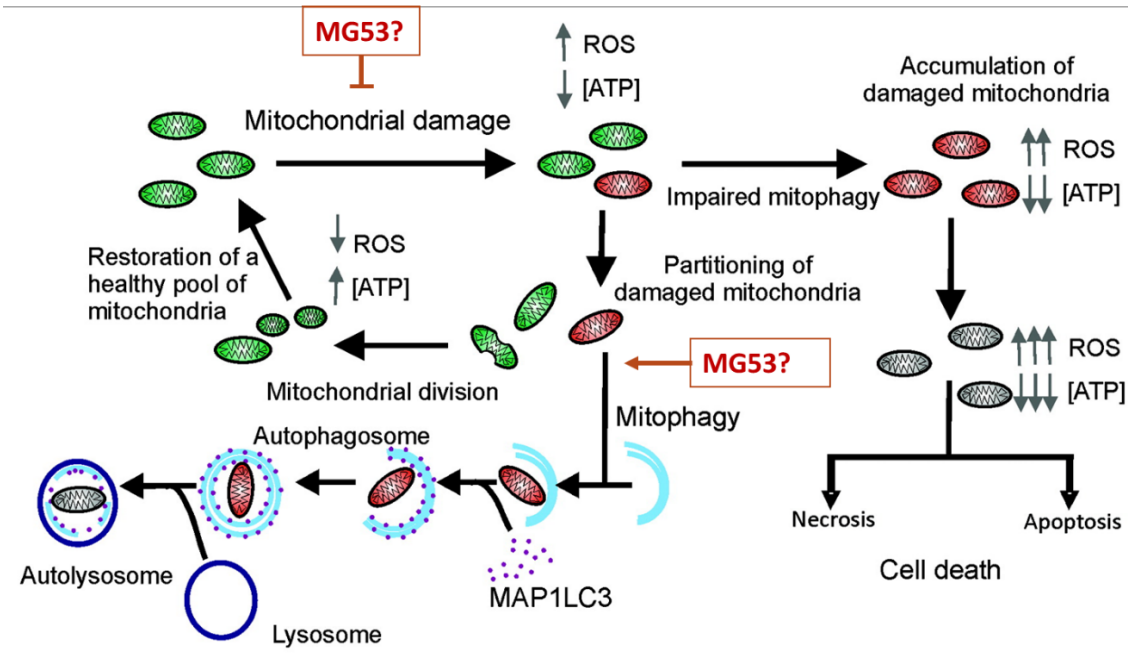

Figure 3 MG53 in Mitophagy Hypothesis

Figure adapted from Dolman et al. 2013 with permission.

TRIM50: A Mediator of Gastric Acid Secretion

TRIM50 is another TRIM protein who's non-E3ubiquin ligase function is better understood than its ligase function. TRIM50 was first identified by Micale et al in 2008 associated with their research into Williams-Beuren syndrome [68]. Williams-Beuren Syndrome is a genetic disorder where a small region of the 7th chromosome is has a microdeletion of approximately 23 genes proteins such as elastin, syntaxin 1, and TRIM50 [68, 69]. Deletion of these genes causes symptoms such as joint laxity, low muscle tone, hypercalcemia, kidney abnormalities, and developmental disorders, amongst other symptoms. The characteristic elfin-like craniofacial abnormalities have been

associated with the deletion of general transcription factor II-I gene family including repeat domain-containing protein 1 gene (GTF2IRD1) . The supravalvular aortic stenosis, hypertension and abnormalities in connective tissue has been clearly linked to the deletion on elastin (ELN) Glucose intolerance has been associated with deletion of syntaxin 1A (STX1A). TRIM50 is one of several other identified proteins deleted in Williams-Beuren syndrome, however its involvement in the pathologies of this disorder have not yet been characterized.

Like MG53, TRIM50 contains a PRY/SPRY domain and is relatively similar in sequence to MG53, diverging from the rest of the TRIM family proteins together before separating into two distinct proteins [70]. Unlike MG53, TRIM50 is mainly expressed in the parietal cells of the stomach and does not participate in plasma membrane repair. Rather, removing TRIM50 expression from mice resulted in dysfunction of gastric acid secretion. Trim50 -/- mice displayed an alkaline gastric pH without changes in H^+/K^+ ATPase (ATP4A) expression or activity [70]. Additionally, after stimulation with histamine, the luminal membrane of the parietal cells became disordered, with truncated microvilli and multilamellar membrane complexes, suggesting a possible dysregulation in the ATP4A-associated vesicle trafficking in trim50 -/- mice.

Gastric acid secretion is a highly regulated biological process required for the proper digestion of food and absorption of essential nutrients. When this process is dysregulated, several outcomes occur. Either patients secrete too much acid and experience painful symptoms like peptic ulcers and GERD, resulting in the development of cancers such as esophageal or peptic cancer, or patients do not secrete enough acid

resulting in iron deficiency anemia, hypochloridria, and or bacterial overgrowth [71, 72]. Current therapy for dysregulated acid secretion involves either ingesting products like TUMS or Rolaids to temporarily neutralize the highly acidic environment of the stomach, or take H2 receptor blockers, or proton pump inhibitors (PPIs) for more chronic conditions. In the past several years, there has been some controversy over the safety of long-term use of PPIs for GERD [73–75]. Some studies have indicated long-term use of PPIs results in hypocalcemia or hypomagnesemia which could lead to an increased chance of bone fractures, dementia like Alzheimer's disease, and renal complications [76]. However, although many of these studies have limitations that cannot definitively determine a relationship between PPI use and these disorders. **To avoid more controversy, learning more about the mechanisms that mediate gastric acid secretion at a cellular level may provide new targets for managing hypersecretion disorders, providing alternatives to PPIs.**

Overview of Proposed Hypotheses

Ischemic heart diseases like myocardial infarctions (MIs), also known as heart attacks, have a heavy burden on morbidity and mortality world-wide [77]. Indeed, Coronary heart disease affects approximately 635,000 Americans a year and about 300,000 with a recurrent coronary attack [78]. MIs are caused by a cessation of blood flow to an area of the cardiac tissue, preventing oxygen and nutrients getting to the blocked area. This causes oxidative stress which, in turn, prevents energy generation by the cellular organelle mitochondria. Lack of energy production and an increase in ROS

secretion from the damaged mitochondria results in signaling for cell death and scarring in the blocked tissue. Current treatments for myocardial infarctions involve clearing the blockage then a lifetime of anticoagulants, beta blockers, calcium channel blockers, cholesterol-lowering medications and/or vasodilators, to name a few [79]. These treatments help maintain heart function with the remaining healthy tissue, but do not address the damaged and scarred tissue. A goal for helping patients with MIs is to help heal the damaged tissue before cell death and scarring occurs, restoring or preserving function without the need for long-term medications. **In this context, the first goal of this dissertation is to assess the localization of MG53 around mitochondria after oxidative damage in hearts/cardiomyocytes to improve our understanding MG53-mediated cardioprotection.**

Dysregulation of gastric acid secretion is often associated with the occurrence of peptic ulcers in an overly acidic gastric environment and nutrient deficiencies in an overly alkaline gastric environment. Since TRIM50 is involved in acid secretion, a major component of digestion, it is imperative that we understand exactly how TRIM50 is involved in vesicle trafficking and acid secretion to better aid in the understanding of how Williams Syndrome patients are affected by this deletion. **In this context, the second goal of this dissertation is to clarify how TRIM50 mediate gastric acid secretion.**

Currently, there is a gap in knowledge about the functions of the PRY/SPRY domain in many TRIM proteins containing this domain. Recently, Fusco et al. provided some clue to the function of the c-terminal SPRY domain of TRIM50. In 2012, Fusco et al. showed TRIM50 is a component of aggresomes with HDAC6 and p62/Sequestosome

1 in mouse embryo fibroblasts [80]. A polyubiquitin CO-IP in normal and -/- SH-SY5Y cells with MG132 indicated TRIM50 an important component of aggresome clearance [80]. TRIM50's interaction with HDAC6 lead Fusco et al. to discover acetylation of TRIM50 lysine 372 by the p300 acetyltransferase and that this acetylation regulates TRIM50s E3 ubiquitin ligase function as a regulator of proautophagic protein Beclin 1 [80–82]. From this evidence, it is reasonable to conclude there may be other factors within the PRY/SPRY domain that mediate MG53's membrane repair function.

Therefore, the third goal of this dissertation is to determine whether the divergent PRY/SPRY domain of MG53 sufficient to provide membrane repair functionality to another TRIM RBCC domain through the creation of a TRIM-MG53 chimera.

Chapter 2. Materials and Methods

Purification and quality control of rhMG53

High quality recombinant human MG53 (rhMG53) was produced through *E. coli* fermentation as previously described [36]. Quality of the purified protein was determined via western blot for size and purity. A lactose dehydrogenase (LDH) release assay was used to determine functionality of each batch of protein using a microbeads damage model as previously described [36] as well as briefly detailed below.

Porcine Model of Angioplasty-Induced Myocardial Infarction

Chinese experimental miniature swine were provided by Beijing Experimental Animal Reproduction and Regulation Center (Grade II, Certificate No. Jing-030). All porcine experiments in this study were performed in accordance with China Academy of Chinese Medical Sciences Guide for Laboratory Animals that conforms to the Guide for the Care and Use of Laboratory Animals published by the U.S. National Institutes of Health. Experimental pigs underwent balloon inflation of the left anterior descending (LAD) coronary artery according to established methods as described 6. Administration of rhMG53 at different times of experimental interventions was achieved through the jugular vein.

Murine Model of Myocardial Infarction

All murine experiments in this study were performed in accordance with The Ohio State University IACUC-approved protocols. The mg53-/- mice were generated as described 4 and wild type littermate mice were used as indicated. Saline or 1mg/kg rhMG53 dissolved in saline was injected via the jugular vein 10 minutes prior to induction of myocardial infarction via LAD ligation. Ischemia was maintained for 60 minutes. After ischemia, another 1mg/kg of rhMG53 was injected via the jugular vein and the mouse recovered for 6 hours before cardiac tissue collection for histology, immunofluorescent staining and biochemical analysis.

Myocardial Tissue Pathology

Porcine and Murine tissue samples were embedded in paraffin, sectioned (5 μm thickness), and stained with antibodies against MG53, COXIV (Cell Signaling Technologies, 11967S), and/or cleaved caspase 3. Cleaved caspase 3, MG53 and COXIV stained slides were imaged on a Zeiss 780 Confocal microscope using Zen 2012 software (Zeiss). Colocalization and fluorescent intensity was quantified using FIJI (ImageJ).

STORM Single Molecule Imaging

HeLa cells plated on 35mm glass bottom dishes (MatTek Corp) were transfected with myc-MG53. Cells were fixed and background signal was reduced with 3% paraformaldehyde and 0.1% glutaraldehyde for 10 minutes. Cells were blocked with 3% IgG-Free BSA and 0.2% Triton X-100 in BSA for 1hr at room temperature and

subsequently probed with 914 antibody directly conjugated to AlexaFluor-647 at approximately 1-2 fluorophores per antibody for 30 minutes at room temperature. After washing, antibodies were secured in a post-fixation step using 3% paraformaldehyde in PBS for 5 minutes. After staining, cells were immersed in 1mL STORM Imaging Buffer (10% glucose, 50 mM Tris pH 8.5, 10 mM NaCl, 14mg Glucose Oxidase, 50µL 20mg/mL catalase, and 1Xβ-mercaptoethanol (Sigma Aldrich)). The dish was sealed with parafilm to reduce oxygen entry into the dish. Stochastic "blinking" of the fluorophores was achieved through a brief bleaching step before temporal data was collected under TIRF conditions. Image reconstruction was performed through a program built in MATLAB as described previously [83, 84].

HL-1 Cell Oxidative Damage Models

HL-1 cardiomyocytes, a kind gift from Dr. W. Claycomb (Sigma, SCC065), were cultured at low passages (7-20) according to established protocols 12,13. For H_2O_2 damage, HL-1 cells were subjected to 300uM H_2O_2 in unsupplemented Claycomb media for 1h and recovered in unsupplemented Claycomb media with either 10ug/mL BSA or rhMG53 for 2h. For a hypoxia/reoxygenation model, we adapted the protocol for hypoxia, energy depletion, and acidosis (HEDA) from Åström-Olsson et al. 14. Briefly, HL-1 cells were immersed in PBS pH 6.7 without glucose, Mg^{2+} or Ca^{2+} and placed in a sealed chamber gassed with 5% CO_2, 1% O_2, and balance N_2 to establish the HEDA environment. Control cells were incubated in a Balanced Salt Solution (BSS) (140mM NaCl, 2.8mM KCl, 2mM $MgCl_2$, 1mM $CaCl_2$, 12mM Glucose, 10mM HEPES, pH 7.4) in a regular tissue culture incubation chamber at 5% CO_2 and ambient air. HEDA-treated

cells were recovered in the BSS solution for 1h. For each treatment group, either 10μg/mL of BSS or rhMG53 was added to the media before the 24h incubation.

Confocal Microscopy

HL-1 cells cultured on 35mm glass bottom dishes were assessed for mitochondrial health using the fluorescent dyes TMRE (company and number) and MitoSOX Red (Invitrogen, M36008). Briefly, dyes were dissolved in DMSO. Cells were incubated with either 50nM TMRE or 5μM MitoSOX Red for 15min at 37C protected from light. Excess dye was rinsed away with BSS then immersed in BSS. Images were collected with a Zeiss 780 confocal microscope and analyzed in FIJI, measuring the integrated density of each cell. Integrated density of each cell divided by integrated density of the background was used for quantification.

Mitochondrial morphology was assessed using FIJI by performing a Z-projection of the z-stack of images. The image was processed by using the FIJI processes of background subtraction function which utilizes a 50μm rolling ball radius, followed by CLAHE (contrast limited adaptive histogram equalization), median filter at 1.5. Finally ridge detection with width estimation was then performed to determine the shape and size of the mitochondria.

Lipid Binding Assay

rhMG53 was applied in increasing concentrations to the ELISA Snoopers® (Avanti Polar Lipids) lipid strips. ELISAs were performed according to manufacturer's protocol. MG53 5259 antibody conjugated to biotin was used for detection. Signal was

developed using Streptavidin-HRP detection antibody and TMB Substrate Reagent (BD OptEIA, 555214) and quantified using a Flex Station III plate reader.

Western Blotting

Twenty-four hours after surgery, proteins from different area of porcine myocardium were collected and diluted into 0.5 mg protein/mL for the measurement of pro-survival pathway proteins. Protein content was determined with BSA as a standard according to Bradford assay. Protein samples (20 μg/lane) were separated by sodium dodecyl sulfate-polyacrylamide gel electrophoresis and were transferred to PVDF membranes (Millipore, Billerica, MA) through electroblotting. Blots were probed with antibodies against GFP (Abcam, ab13970), MG53 (914), Drp1 (Santa Cruz, sc-271583), Mfn2 (Santa Cruz, sc-515647), GAPDH (CST, 2118S), alpha tubulin (Abcam, ab6160), COX IV (CST, 11967S), and Cytochrome C (CST, 4280). The blots were developed by chemiluminescence using SuperSignal west femto maximum sensitivity substrate (Thermo Fisher Scientific, 34095) using a Bio-Rad Chemidoc Imaging System. Bio-Rad Image Lab™ Version 6.0 software was used to calculate the numerical value of every blot.

Gastric Gland Isolation

Gastric glands were isolated from trim50 -/- and WT mice following an amended protocol as described previously [85–87]. Briefly, mice were fasted overnight and sacrificed via CO2 asphyxiation. The circulatory system was perfused with 10mL warmed and oxygenated PBS with 1mM MgCl2 and 1mM CaCl2 to remove blood from

the organs. The stomach was removed and opened along the lesser curvature to expose the rugae and rinse out any remaining contents in the stomach with more warmed, oxygenated PBS, then in warmed, oxygenated MEM (company). The stomach was minced into small pieces and placed into a 25mL conical flask with 10mL Digestion Media (MEM with 100mM HEPES pH 7.4, 0.1% BSA, 1% Gentamycin, 10mg/mL Collagenase D). The tissue was incubated at 37C for 30 minutes shaking at 155rpm. After digestion, FBS was added for a final 1% concentration to inhibit the collagenase and the tissue was shaken vigorously to dissociate the intact glands from the rest of the tissue. The gland solution was centrifuged at 200xG for 3min to pellet the glands. The pellet was gently resuspended in Gland Rinse Media (DMEM/F12 1:1 with 0.1% BSA, 1% Pen/Strep, 1% Gentamycin, 250mM DTT) and glands were separated from remaining tissue by filtration through a 100µm cell filter. The glands were allowed to gravity settle for 20 minutes before removing the rinse media and resuspending in Gland Culture Media (DMEM/F-12 1:1 with 0.1% BSA, 1% Gentamycin, 100ng/mL EGF, 1x ITSS, 4ng/mL Hydrocortisone, 10mM HEPES-Na+, 0.5% Pen/Strep) for plating on Matrigel-coated 35mm glass bottom dishes. Glands were kept at 37C with 5% CO_2 for up to 1 day.

Intracellular Gastric Acid Secretion Analysis

Primary isolated gastric glands were loaded with 10µM BCECF-AM (Thermo Fisher Scientific, B1150), a ratiometric fluorescent pH indicator at 37C, CO2-free in HEPES solution (145mM NaCl, 3mM KCl, 1mM $CaCl_2$, 1.2mM Mg_2SO_4, 5mM Glucose, 32.2mM HEPES (acid), pH 7.4) for 15 minutes. Excess BCECF-AM was rinse 3x in

HEPES solution. The dish containing the loaded glands was placed on a PTI Easy Ratio Pro microscope system (Horiba Scientific) and measured at 440 and 490nm emission with approximately 20ms between channels. Glands were perfused with HEPES solution for 2 minutes, then acid loaded with NH4Cl solution (3mM KCl, 1mM CaCl2, 1.2mM Mg2SO4, 5mM Glucose, 32.2mM HEPES, 125mM NMDG-Cl, 20mM NH4Cl, pH 7.4) for 5 minutes. After acid loading, the glands were perfused with 0 Na+ buffer (3mM KCl, 1mM CaCl2, 1.2mM MgCl2, 5mM Glucose, 32.2mM, 125mM NMDG-Cl, pH 7.4) for 10 minutes. Cells were returned to HEPES solution for 2 minutes before being perfused with the High K+ Calibration solution (105mM KCl, 1mM CaCl2, 1.2mM MgSO4, 32.2mM HEPES, 10mM Mannitol, 10ug/mL nigericin) at pH 7.0. pH measurements were determined using the pH 7.0 calibration measurement against a calibration standard performed each day with one of the dishes ranging from pH 5 to 9 to make a sigmoidal curve.

Live Cell Imaging of Vesicle Movement

TMK-1 cells, a kind gift from Dr. Sakamoto Naoya were transfected with mCherry-TRIM50. Movies of TRIM50-associated particle motion was collected with confocal microscopy at 0.5 frames/sec. Percentage of particles with directed motion was determined using a MATLAB-based, analysis program written in our lab. Output is in the percent of particles that move in a directed motion.

Chimeragenesis

GFP-TRIM50/MG53 chimera was constructed by using PCR to produce MG53's c-terminal domain including cysteine 242 with the primers in Table 2, adding MfeI and BspEI digestion sites. GFP-TRIM50 plasmid was digested with BspEI and MefI, creating a break in the TRIM50 sequence at leucine 285, just before the PRY/SPRY domain. The constructs were verified through PCR using a TRIM50 n-terminal primer and the MG53-MfeI primer and run on a gel. To ensure the base pair sequence was correct without the addition of a premature stop codon, the plasmid was verified through sequencing using the Ohio State University Comprehensive Cancer Center Genomics Sequencing Resource.

Table 2 Primer sequence for chimeragenesis

Primer Name	**Sequence**
BspEI-MG53	5'-gcagTCCGGAcacagacagaattcctcatgaaatt-3'
MG53-MfeI	5'-gcagCAATTGGTTATCTAGATCAGGCCTGTTC-3'

Cell Poking Assay

HeLa cells were plated on a low-walled glass bottom dish and transfected with GFP-TRM50/MG53. Media was changed to a warmed 1x BSS solution (NaCl, KCl, MgCl2, 1mM CaCl2, 20mM Glucose, HEPES, pH 7.4).Cells were damaged by

mechanical quick penetration of a microcapillary needle and signal motion was collected using a Bio-Rad Confocal Microscope.

LDH Release Assay

HeLa cells were transfected with either control GFP-C1, GFP-MG53, mCherry-TRIM50, or GFP-TRIM50/MG53 chimera. After expression was visible, cells were trypsinized and approximately 300,000 cells were added to each well of a 96-well dish in 50uL of PBS. Each construct had 3 wells and either, PBS with 2mM CaCl2, PBS with 2mM CaCl2 and 1% Triton X-100, or PBS with 2mM CaCl2 and glass microbeads (Sigma, G4649-100G). The plate was shaken vigorously on an orbital shaker at 100prm for 6 minutes, then centrifuged at 3,000 xG for 5min to pellet cells and beads. 50uL supernatant was transferred to a fresh 96 well plate and assayed for LDH concentration following the kit's protocol (Clontech, MK401).

Urinalysis

Mice were housed in urine collection cages overnight with free access to water and food. Urine was collected for 12 hours and subjected to protein analysis via the Bradford method (Bio-Rad, 500-0006) and Creatinine content via the Jaffe method following the QuantiChrom™ kit protocol (BioAssay Systems, DICT-500).

Statistical Analysis

Data was analyzed by several statistical methods (e.g., paired or unpaired t-tests, ANOVA, etc.) using commercial Prism software (GraphPad Prism 8). Data were presented as means ± SD. For comparisons between two groups, significance was determined by Student t-test parametric analysis. For comparison of multiple groups, multifactorial analysis of variance (ANOVA) was used to determine statistical significance. Corrections, such as Brown-Forsythe or Welch's correction, were used if there was a difference in variance between groups. For all statistical tests: *$p<0.05$, **$p<0.01$, ***$p<0.001$, ****$p<0.0001$

Chapter 3. MG53 Mediates Survival of Cardiac Tissue Through Maintenance of Healthy Mitochondria

Introduction

With the increasing prevalence of obesity and unhealthy lifestyles, ischemic heart disease remains a major cause of mortality and morbidity world-wide, responsible for approximately 1/3 of all deaths in individuals over 35 years [77]. Ischemic injury causes a loss of healthy mitochondria, resulting in loss of energy production and either necrosis or apoptosis [88]. Cells can undergo a process called mitophagy to remove damaged mitochondria and preserve healthy mitochondria to promote cell survival. Canonically, proteins PINK1 and Parkin are recruited to promote ubiquitin-tagging of damaged mitochondria, signaling for lysosome formation and breakdown of the damaged mitochondria [63, 65]. However, there are many other ubiquitin ligases located on and around the mitochondria involved in the mitophagy process.

As of yet, MG53's link to mitochondrial protection remains tenuous at best, with only a few studies showing overexpression of MG53 preserving mitochondrial membrane potential or increases in expression of LC3 and Tom20 via co-localization [89, 90]. These papers, although important in indicating a potential interaction of MG53 with the mitochondria, only show correlations between MG53 and mitophagy. Here, I demonstrate that in addition to cell membrane repair, exogenous rhMG53 protects cells

from ischemic damage by maintaining mitochondrial function by mediating oxidative-stress induced mitophagy. In particular, we show MG53's protection of heart tissue after a myocardial infarction is a two-fold mechanism of plasma membrane repair, as previously reported [39, 41], as well as preserving mitochondrial function to maintain energy production and reduce mitochondrial ROS secretion into the cell cytoplasm.

Results

MG53 oligomerization increases after oxidative stress

Early studies on MG53 established it will dimerize or trimerize after changes in oxidative state and speculated these changes enable MG53 to form membrane repair patches. To further clarify MG53's polymerization after oxidative stress, HeLa cells underwent normoxia or hypoxia and stained for MG53 using our homemade 914 antibodies directly conjugated to AlexaFluor-647. Superresolution single-molecule fluorescence microscopy using the STORM method revealed the expected dimerization or trimerization of MG53 under normal conditions. However, four to five MG53 proteins will oligomerize in large clusters after hypoxia treatment(Figure 4).

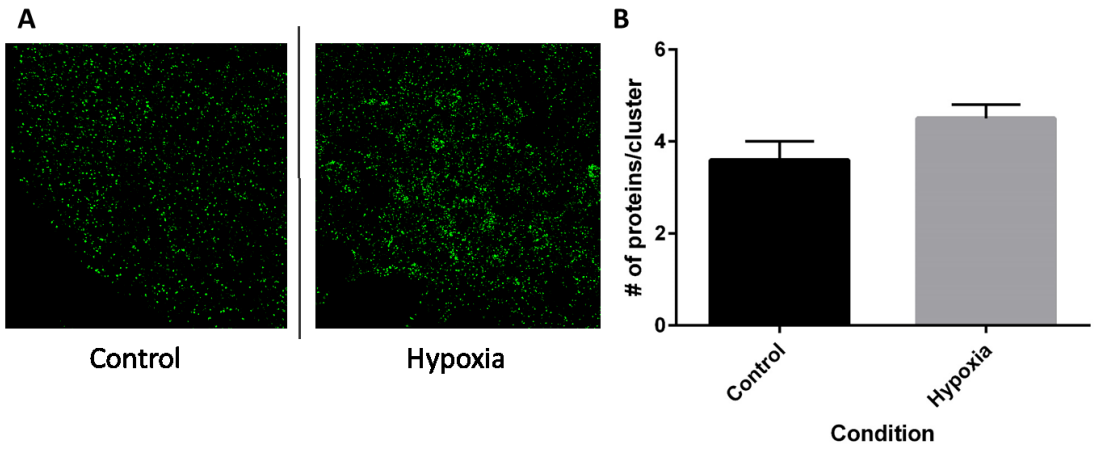

Figure 4 MG53 forms larger oligomers in response to oxidative stress

(A) STORM image of HeLa cells transfected with MG53. Hypoxia conditions were created by placing transfected cells in a sealed chamber and gassed with 1%O2, 5% CO2 , and 94% N2 for 10 minutes before the chamber was sealed and incubated at 37C for 24 hours before imaging. (B) Quantification of MG53 density in response to hypoxia condition. Control = 3.6 +/- 0.4 particles per cluster. Hypoxia = 4.5 +/- 0.3 particles per cluster. In all cases, n=10 cells. p = 0.0003

MG53 translocates to cardiac mitochondria after oxidative stress

In cardiac tissue, endogenous MG53 and exogenous rhMG53 typically localizes to the intercalated discs, an area of constant low-level plasma membrane microtears as the heart expands and contracts for each beat [41]. Because there is an apparent change in localization of MG53 to COX IV after high-fat diet induced oxidative stress injury in skeletal muscle, we hypothesized exogenous MG53 will also translocate to the mitochondria in cardiomyocytes after ischemia/reperfusion injury. To address whether MG53's localization changes in cardiac tissue, we subjected Chinese experimental miniature swine to myocardial infarction and recovery. As seen in Figure 5A (top) MG53 localizes to the intercalated discs of the cardiomyocytes. After myocardial infarction injury, MG53's intracellular distribution appears to change, partially co-localizing with COX-IV, a subunit in the terminal enzyme complex of the electron transport chain (Figure 5A (bottom) and B). In order to examine the purpose of MG53 recruitment to the mitochondria, we used the HL-1 immortalized mouse atria-derived cardiomyocytes for *in vitro* studies.

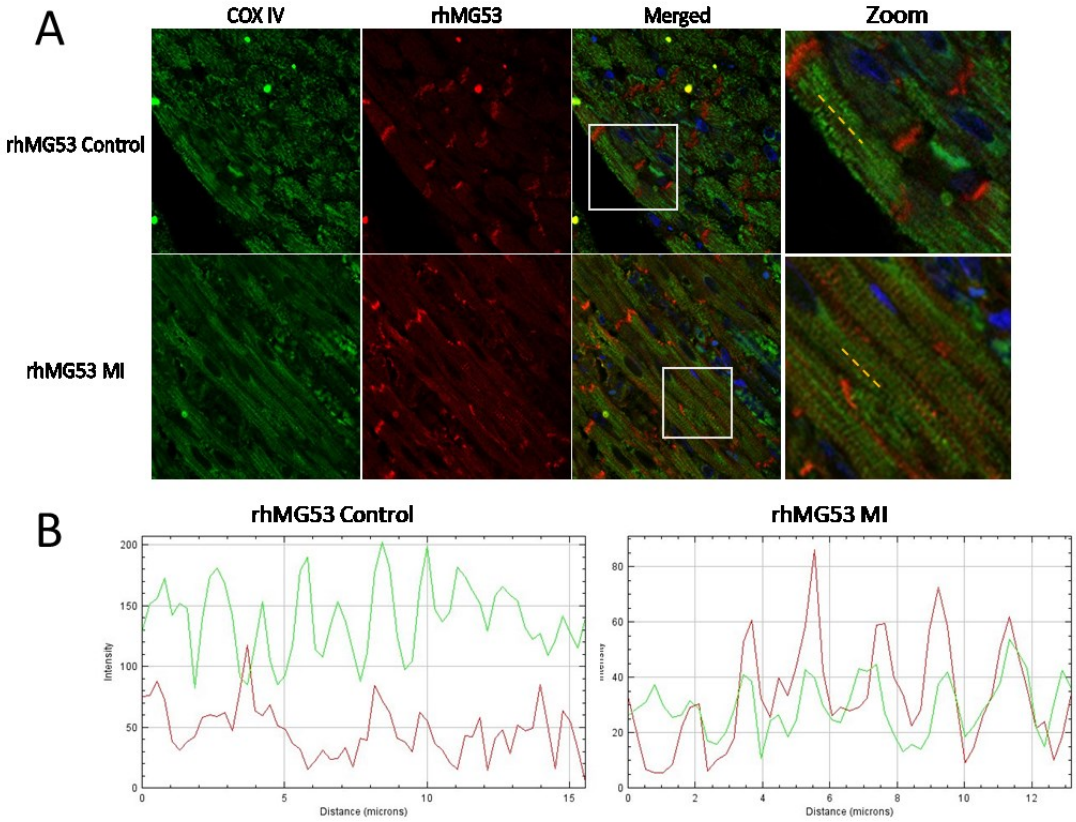

Figure 5 MG53 Translocates to Mitochondria in Cardiac Tissue After Myocardial Infarction Damage

(A) Representative images of pig hearts treated with rhMG53 with or without myocardial infarction stained for DAPI (blue), COX IV (green) and rhMG53 (red). (B) Profile plots of images as indicated with yellow dotted line in the zoom panels.

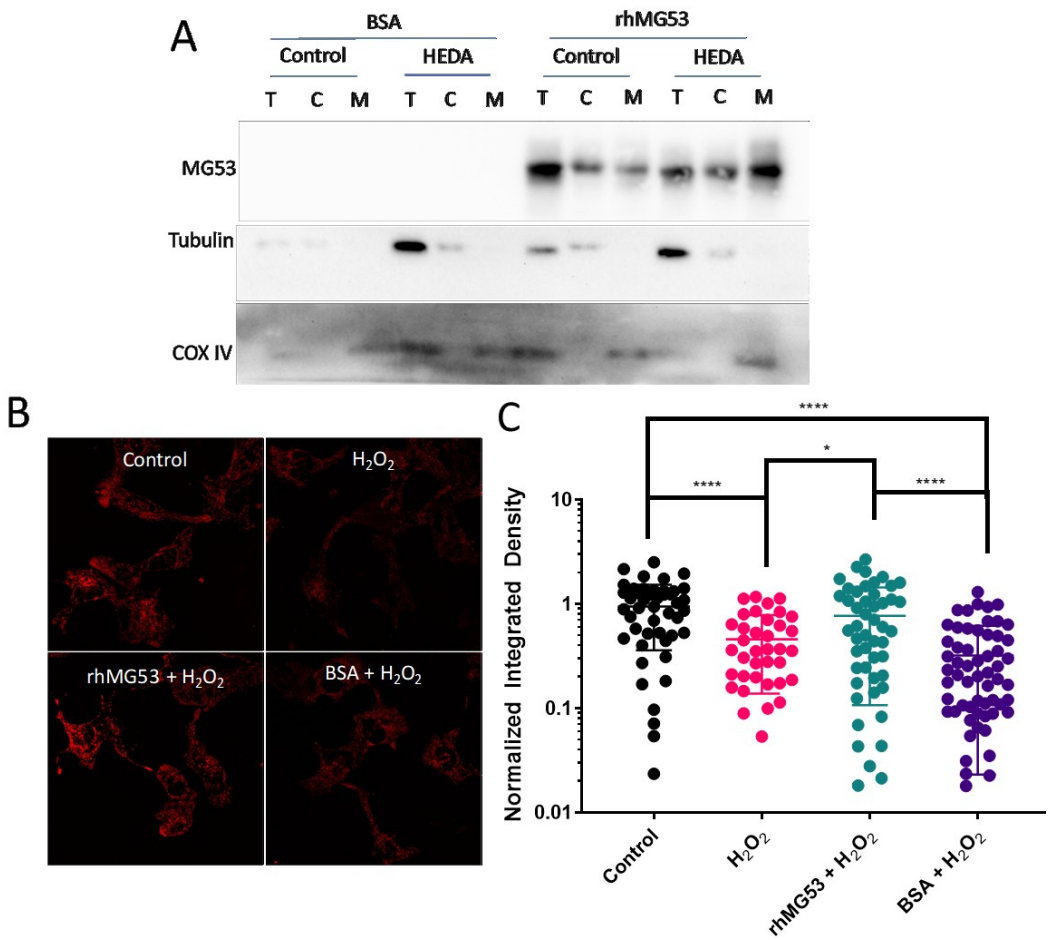

Figure 6 rhMG53 Enters HL-1 Cells to Preserve Mitochondrial Membrane Potential

(A) HL-1 cells were subjected to either normoxia or HEDA damage with either 10μg/mL BSA or 10μg/mL rhMG53. Cells were fractionated into a cytoplasmic and mitochondria fraction, indicated by the presence of tubulin or COX IV. (B) HL-1 cells were plated on 35mm glass bottom dishes and underwent either normoxia or HEDA damage with either 10μg/mL BSA or 10μg/mL rhMG53. Cells were stained with TMRE for mitochondrial membrane potential. (C) Quantification of TMRE normalized to average intensity of control. n=3 dishes/treatment

MG53 reduces markers of mitochondrial damage

After establishing MG53 localization around mitochondria after oxidative stress, we recapitulated the environment that would normally surround cardiomyocytes during myocardial infarction *in vitro* using a **h**ypoxia, **e**nergy **d**epletion, and **a**cidosis (HEDA) model to assess MG53 function at the mitochondria[91].This model recapitulates physiologic changes that occur in the myocardium after ischemia/reperfusion injury. During injury active cells without access to oxygen and energy sources like serum glucose undergo metabolic changes due to energy depletion, reducing ATP production.. Subcellular fractionation of normal and HEDA treated cells revealed an enrichment of MG53 in the mitochondrial fraction (Figure 6A). Using an H_2O_2 model of oxidative stress, MG53 co-localization with the mitochondria prevented loss of mitochondrial membrane potential as revealed by the TMRE intensity preservation as seen in Figure 6B and C.

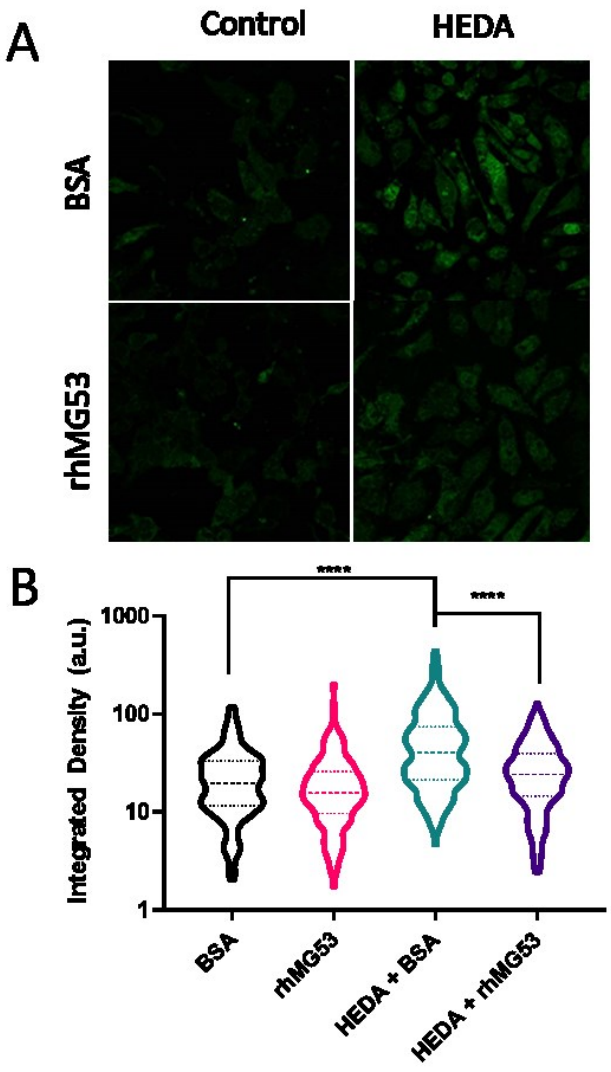

Figure 7 rhMG53 prevents release of superoxides from mitochondria

Representative images of HL-1 cells that underwent normoxia or HEDA treatment with either 10μg/mL BSA or 10μg/mL rhMG53 and stained with MitoSOX Red. (B) Quantification of MitoSOX Red signal. n= 3 dishes/treatment

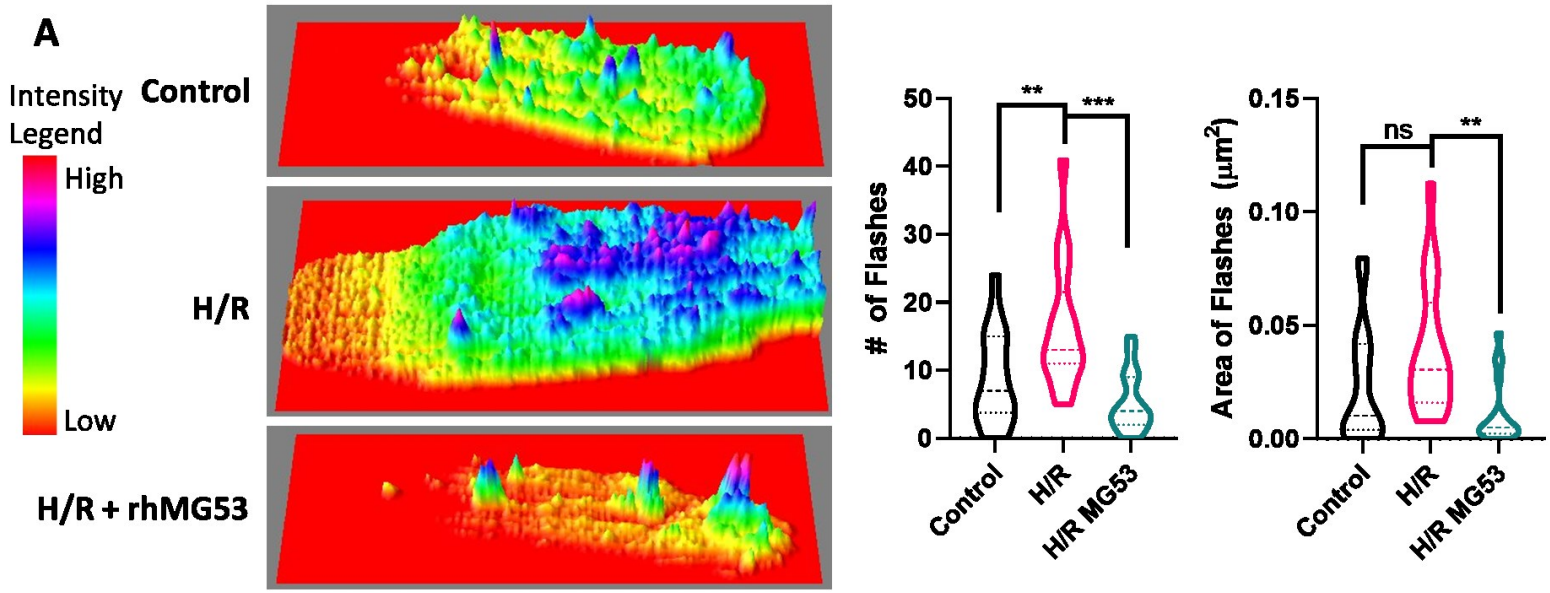

Figure 8 MG53 reduces MitoFlash in isolated cardiomyocytes

Cardiomyocytes from transgenic mice expressing mt-cpYFP underwent normoxia (Control), hypoxia/reoxygenation (H/R), or hypoxia/reoxygenation + rhMG53 treatment (H/R + rhMG53). (A) Representative z-projection images averaging 100frames of live cell imaging after each treatment. (B) Quantification of images counting the number of flashes per cardiomyocyte/cardiomyocyte cluster and the area of each cell/cluster that flashed over 100frames. n = 3 mice, 6 images per mouse.

MG53 prevents the release of superoxide anions after oxidative injury

One of the hallmarks of mitochondrial damage and instigators of mitophagy is an increase in ROS within the cell [60, 61]. HL-1 cells underwent normoxia or HEDA treatment for 24 hours and stained with MitoSOX Red, a cytoplasmic fluorescent indicator that only fluoresces in the presence of superoxide radicals, but not other reactive oxygen or nitrogen species. Figure 7A and B shows treatment with either BSA or rhMG53 under normoxic conditions did not alter release of superoxides from the mitochondria. Cells given BSA during HEDA damage showed a significant increase in MitoSOX Red fluorescent intensity. Treating cells with rhMG53 after HEDA significantly reduced MitoSOX Red fluorescent intensity, indicating either prevention of mitochondrial membrane injury or maintenance of a healthy pool of mitochondria. The reduction in ROS secretion was also seen in an *ex vivo* model using the fluorescent protein cpYFP (Figure 8A). Treatment with rhMG53 reduced the number of ROS flashes as well as the area of each flash (Figure 8B).

Mitochondria preservation is mediated by MG53 interaction with cardiolipin

After mitochondrial damage, cardiolipin gets flipped from the inner mitochondrial membrane to the outer mitochondrial membrane and oxidized as a signal for mitophagy [92, 93]. To determine whether rhMG53 binds to cardiolipin on mitochondria like it does the exposed phosphatidylserine of injured plasma membrane, we reanalyzed the lipid binding properties of rhMG53 to include mitochondria-specific cardiolipin. Lipid dot blot assay shows the expected strong binding affinity MG53 has for phosphatidylserine (PS)

(Figure 9A). However, we also see binding between MG53 and cardiolipin (CL). The binding affinity between MG53 and cardiolipin was assessed using a lipid binding ELISA assay. Figure 9B shows MG53 binds to cardiolipin but not as strongly as it does to phosphatidylserine, similar to the intensity of binding in the dot blot.

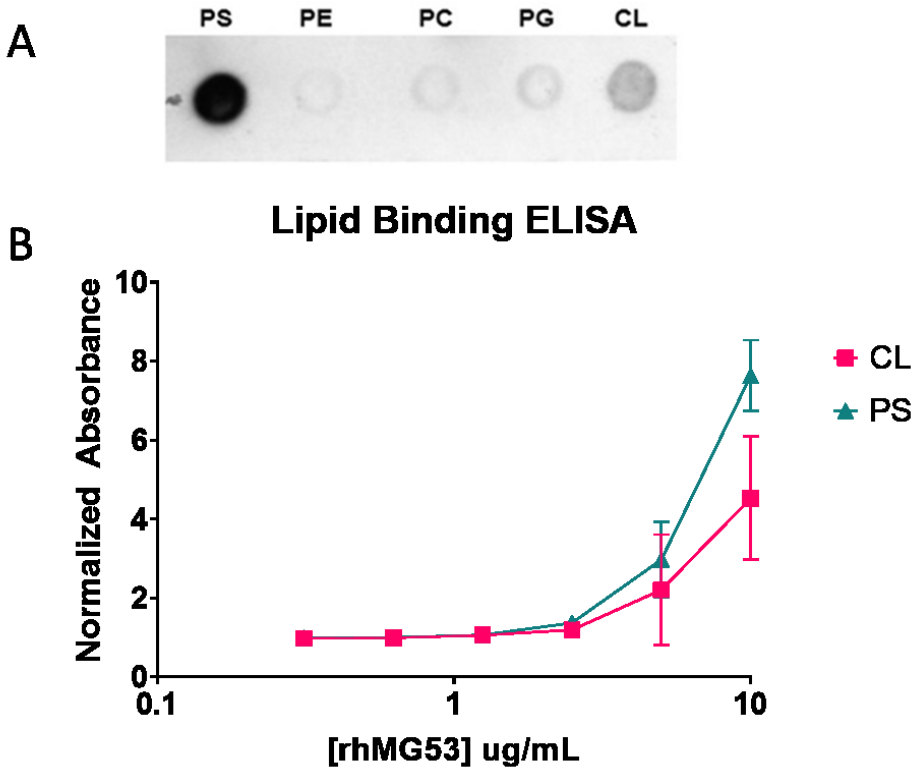

Figure 9 MG53 binds to cardiolipin

(A) Lipid dot blot assay for rhMG53 binding to phosphatidylserine (PS), phosphatidylethanolamine (PE), phosphatidylcholine (PC), phosphatidylglycerol, and cardiolipin (CL). (B) Lipid binding ELISA of rhMG53 to PS and CL. n=3

Discussion

Finding methods of tissue preservation after ischemic events like stroke and heart attack is essential to improving quality of life of surviving patients. Maintaining a healthy mitochondria population after ischemic insult is essential for cell, and consequently tissue, survival. We have previously described how MG53, either endogenous and exogenous an protect cells and tissue from ischemic injury by fixing damage to the plasma membrane [27, 31, 33, 36, 40, 43, 45, 89]. Here, we provide evidence that MG53's ability to improve cell survival and tissue function after ischemic injury is, at least partially, due to its ability to preserve a healthy pool of mitochondria through mitophagy.

We identified exogenous rhMG53 translocates to both plasma membrane and mitochondria after oxidative stress injuries like myocardial infarctions, HEDA, and treatment with H_2O_2. This co-localization of MG53 with the mitochondria was correlated with maintenance of a strong mitochondrial membrane potential (Figure 6) and a reduction in mitochondrial-associated reactive oxygen species leak into the cytoplasm (Figure 7)). Previously, we have shown that MG53 can interact with the lipid, phosphatidylserine, which is exposed from the inner leaflet of the plasma membrane upon damage. Here, we show MG53 can also bind to cardiolipin (Figure 9), a mitochondrial-specific lipid that is flipped from the inner mitochondrial membrane to the outer mitochondrial membrane after oxidative stress. This suggests MG53 may have similar function in mitochondria protection as it does plasma

membrane repair by nucleating lipid rafts to wound sites in the mitochondria through lipid binding to patching damaged membrane to preserve membrane potential.

MG53 is classified as an E3 ubiquitin ligase and, to date, only two targets have been identified: focal adhesion kinase, and IRS-1 [47, 52]. Interestingly, FAK binds to MG53 at the b-box domain and not the PRY/SPRY domain which is predicted to provide specificity to TRIM family proteins. A recent paper by Lijie et al. published in early 2019 indicated MG53 expression is correlated with Ambra1 expression in the skeletal muscle of rats with chronic kidney disease [90]. Ambra1 is a key component of parkin-mediated mitophagy as a regulator of autophagosome formation as an interacting partner with LC3 [94]. Their study suggested MG53 promotes Ambra1 expression and formation of the autophagosome with increased TOM20/LC3 co-localization, markers of mitophagy [90]. In conjunction with the data presented here, MG53 may drive mitophagy by binding to exposed cardiolipin for ubiquitination of currently unidentified mitochondrial membrane proteins to nucleate Ambra1 to the damaged mitochondria for formation of the autophagosome and subsequent degradation of the damaged mitochondria.

Previous studies have shown that the human heart does not express MG53 as strong as rodent hearts, suggesting the need for exogenous application of the protein for cardioprotection [95]. Therefore, this study focused on the application of exogenous MG53 rather than an overexpression of MG53 to assess the possibility of using MG53 as a therapeutic agent for mitochondrial protection as a means for cardioprotection. The ability for exogenous MG53 to enter the cells as seen in the

western blots of Figure 6 and preserve healthy mitochondria is a strong argument for the effectiveness of using MG53 as a therapy for ischemic injury. Using MG53 as a therapeutic agent is likely to be safe as the protein is naturally expressed in skeletal muscle and secreted into the serum via exosomes as a myokine [96]. Additionally, we have developed a mouse model that constitutively overexpresses MG53 in the skeletal muscle and have clearly shown the elevated plasma concentration of MG53 in these mice does not affect glucose or insulin tolerance tests [97].

This study provides a novel mechanism behind how rhMG53 treatment may be a clinically relevant strategy to reduce cardiomyocyte injury and maintain cardiac function in patients after ischemic injury. Indeed, this novel mechanism for MG53's function in the cell goes further to explain the near miraculous cell and tissue preservation after ischemia/reperfusion injury by MG53 seen previously. Understanding more about MG53's interactions with mitochondria could be yet another attractive avenue for the development of MG53 as a therapeutic reagent for regenerative medicine.

Chapter 4: TRIM50's Involvement of Gastric Acid Secretion

Introduction

In an effort to better understand the roles of the PRY/SPRY domain in TRIM family proteins and possibly identify another TRIM family protein involved in plasma membrane repair, our lab identified TRIM50 as the most homologous TRIM family protein to MG53 [70]. Unlike MG53, which is highly expressed in striated muscle, TRIM50's expression appears to be limited to the stomach and testis. Deletion of TRIM50 in a mouse model indicated gastric acid secretion is regulated by TRIM50, however the mechanism behind this is tenuous [70]. Deletion of TRIM50 does occur in patients born with Williams-Beuren syndrome and may be related to nutrient absorption issues with these patients. Understanding how TRIM50 is involved in gastric acid secretion may provide some clues to how we can best treat these individuals. Therefore, the goal of this project is to better understand how TRIM50 regulates secretion in gastric parietal cells. Here, I use a knockout (KO) mouse model of TRIM50 to gain a clearer picture of TRIM50's role in gastric acid secretion.

Results

TRIM50's mediation of intracellular vesicle trafficking

After stimulation with histamine, ATP4A-associated vesicles in gastric parietal cells move in a directed motion on growing actin filaments to merge with the luminal plasma membrane. To determine whether this motion is directly associated with TRIM50 movement in the cell, TMK-1 cells, a human gastro adenocarcinoma-derived cell line with parietal cell-like characteristics [98], were transfected with mCherry-TRIM50 and monitored for directed versus ballistic vesicle movement after treatment with cytoskeletal and molecular motor small molecule inhibitors. Figure 10 shows directed motion of TRIM50-associated vesicles is strongly inhibited by Ciliobrevin D, Nocodazole, and Colchicine, but only mildly inhibited by Cytochalasin D. Ciliobrevin D is a dynein inhibitor, preventing that molecular motor from moving on microtubules. Nocodazole and Colchicine are both inhibitors of microtubule polymerization. Cytochalasin D inhibits polymerization of actin. Together, this data suggests TRIM50-associated vesicles most likely move on microtubules via the dynein molecular motor rather than on the actin cytoskeleton like the ATP4A-associated vesicles.

TRIM50 mediates cytosolic buffering

Previous assessment of TRIM50 on gastric acid secretion monitored pH changes in the luminal stomach contents [70]. Because TRIM50 does not appear to be directly involved with the trafficking of ATP4A-associated vesicles, gastric glands were isolated from TRIM50 WT and KO mice to assess intracellular pH changes which can be

correlated to acid secretion. To assess TRIM50's influence on gastric acid secretion, I used a model of acid loading the cells with NH_4Cl in a sodium-free buffer as depicted in Figure 11. The addition of NH_4Cl outside the cell allows NH_3 (gas) to cross through the cell membrane where it binds with free intracellular H^+ and Cl^- ions to reform NH_4Cl inside the cell. The cell then equilibrates the internal pH to extracellular pH as NH_4^+

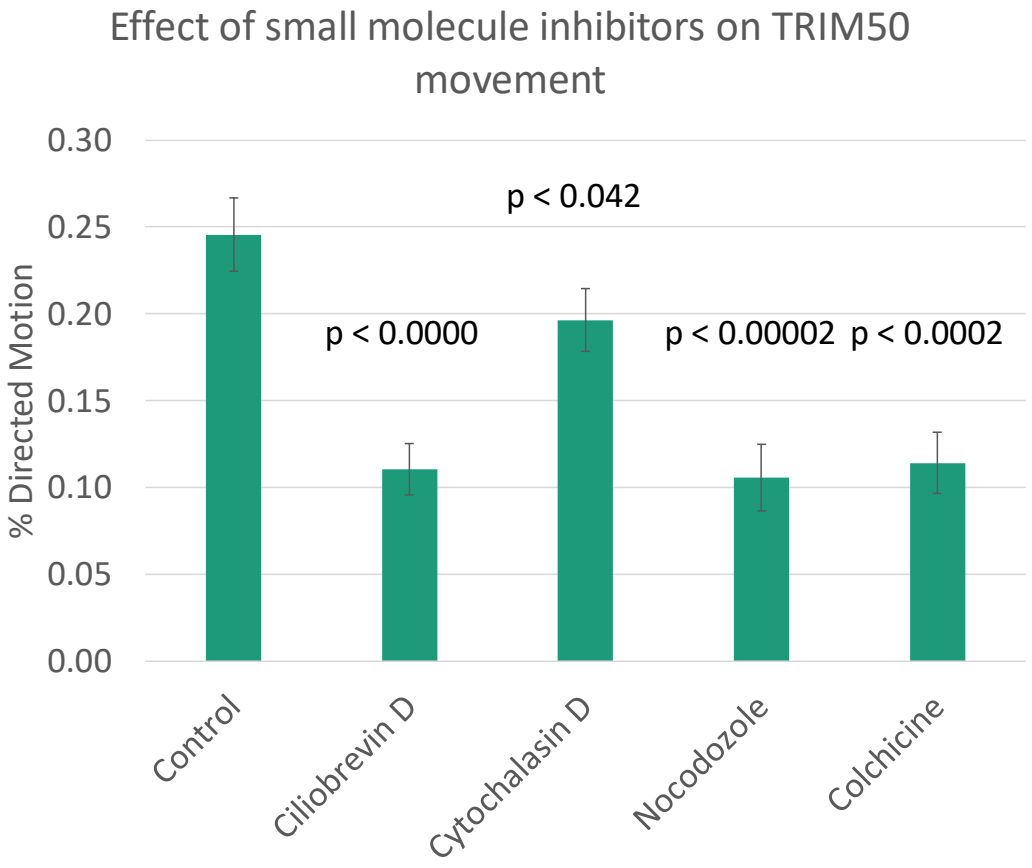

Figure 10 Percent Directed Motion of TRIM50-Associated Vesicles

TMK-1 cells transfected with mCherry-TRIM50 were incubated for 1 hour with 100µM Ciliobrevin D, 1uM Histamine, 5µM Cytochalasin D, 20µM Colchicine, or 5µM Nocodazole and imaged. n>10.

slowly enters the cell through ammonia transporters, establishing an equimolar solution of NH_4Cl inside and outside the cell. After equilibration, removing the extracellular NH_4Cl causes a transient acidification of the cytoplasm of the cell as NH_3 rapidly leaves the cell, moving down its concentration gradient, to restore ammonium equilibrium. H+ ions builds up inside the cell allowing the H^+/K^+ ATPase (ATP4A), stimulated by histamine pretreatment, to pump out the excess H^+ ions, allowing us to measure function of the ATP4A function in WT and KO cells. The cells are maintained in a CO_2, bicarbonate, and sodium-free media to prevent the Na^+/H^+ pumps from removing excess H^+, which would confound the data or extracellular buffering from bicarbonate. Figure 12 shows the average of all trials for gastric glands from WT and KO mice using this model.

Initial assessment of the intracellular pH from the glands of WT and KO mice indicate a dysfunction in intracellular pH buffering. Indeed, baseline acid secretion in gastric glands treated with cimetidine, an H2 histamine receptor antagonist to prevent endogenous stimulation of parietal cells, shows glands from KO mice exhibit intracellular acidosis (Figure 13A). After stimulation with histamine, the intracellular pH of glands from KO mice become alkaline (Figure 13B). Together this suggests TRIM50 may be mediating intracellular buffering rather than directing mediating gastric acid secretion.

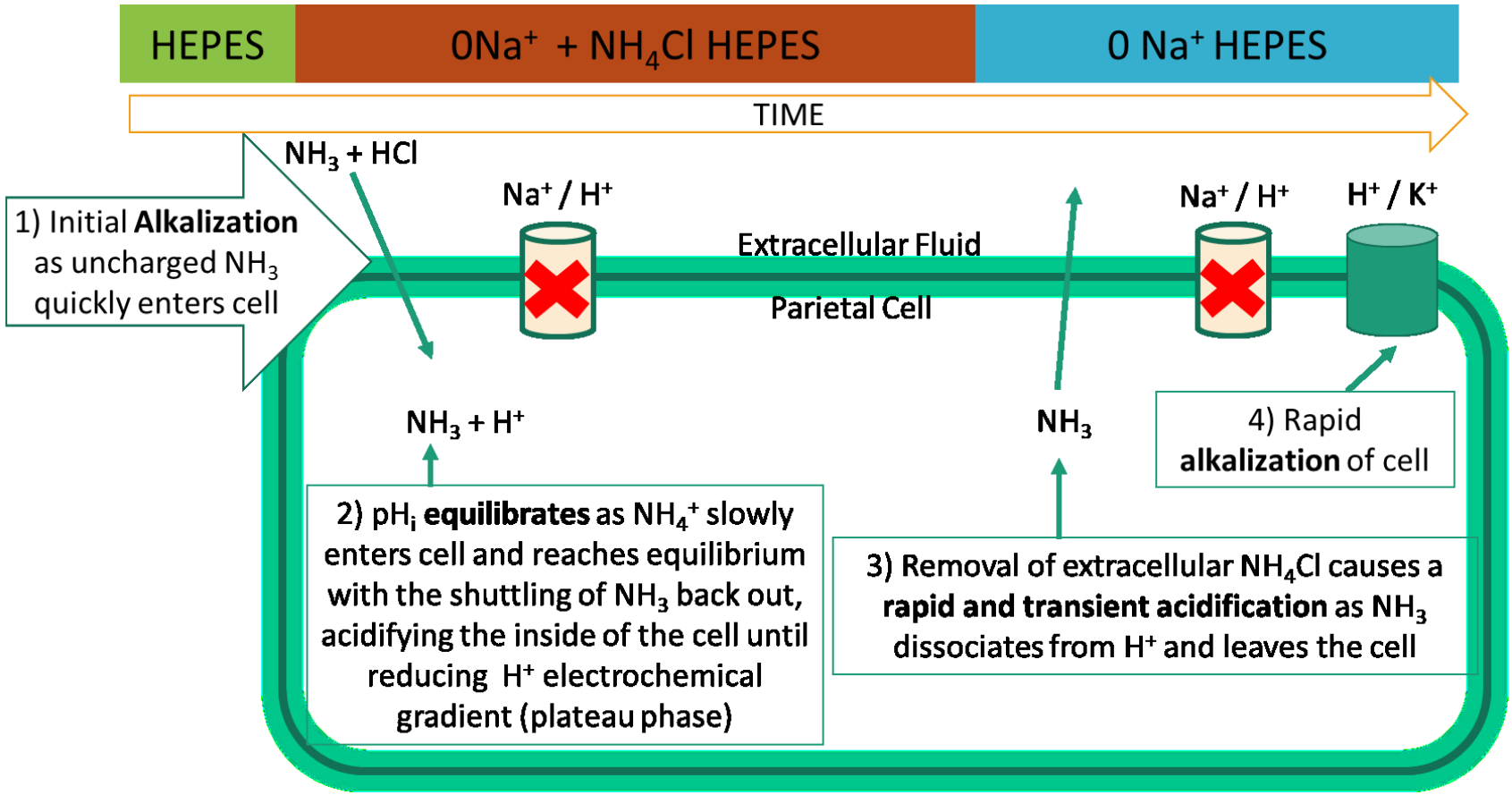

Figure 11 Experimental model to assess gastric acid secretion

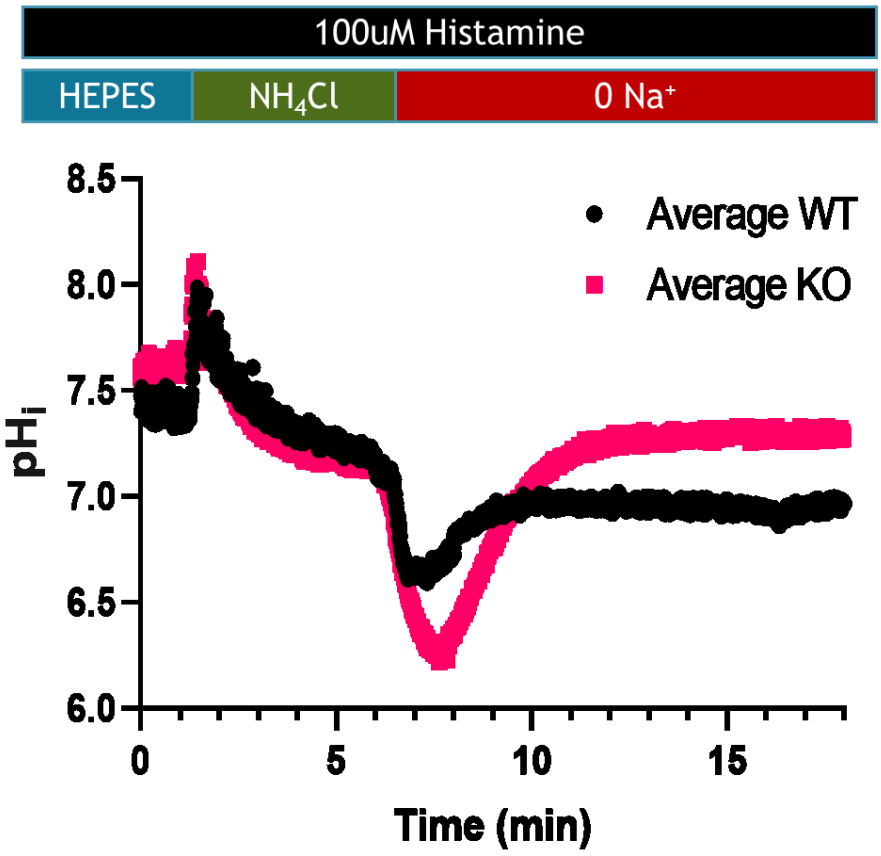

Figure 12 Average traces of gastric acid secretion

Average intracellular pH traces from primary cells from TRIM50 WT (black) and KO (pink) mice pre-treated with 100uM histamine for 1h in HEPES solution.

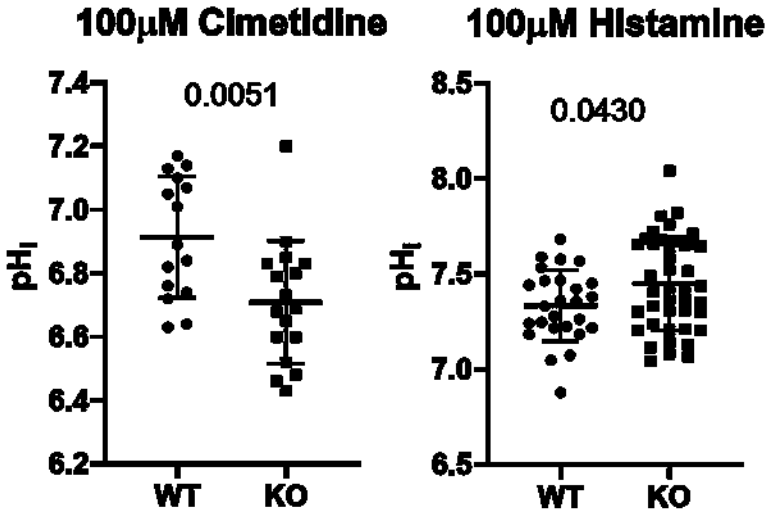

Figure 13 Effect of TRIM50 on basal intracellular pH

Gastric glands from TRIM50 WT and KO mice were pretreated for 1 hour with either 100μM cimetidine, an H2 histamine receptor antagonist, to prevent acid secretion stimulation of the glands from endogenously secreted histamine or 100μM Histamine to induce gastric acid secretion. Glands were derived from at least 3 different mice.

The experimental model used here enables us to determine the buffering capacity of the cell at the transient acidification step upon removal of extracellular NH_4Cl. Before removal of the extracellular NH_4Cl, we see in Figure 13 NH_4^+ and NH_3 are in equilibrium both inside and outside the cell since the internal pH of the cell stabilizes. Because NH_3 gas leaves the cell immediately upon removal of extracellular NH_4Cl, we can calculate the mean intrinsic buffering power (β) of the cell:

$$\beta = \frac{\Delta[NH_4^+]_i}{\Delta pH_i}$$

Equation 1

, where ΔpHi is the total change in internal pH after removing the extracellular NH_4Cl and $\Delta[NH_4^+]_i$ is the change in intracellular ammonium concentration [99]. This can be calculated by:

$$[NH_4^+]_i = 19.37 * 10^{pH_0 - pH_i} mM$$

Equation 2

, where 19.37 is derived from the pK for NH_4^+/NH^3 at an extracellular pH (pH_o) of 7.4 and a starting extracellular concentration of 20mM NH_4Cl [99]. Using this equation, Figure 13 shows parietal cells from TRIM50 KO mice have a significantly reduced buffering power compared to WT cells.

Finally, using this experimental model, we can assess the effect of TRIM50 on ATP4A-associated vesicle translocation and pump function in stimulated parietal cells. Figure 14 measures the change in pH_i over time as the cell pumps the excess H^+ ions out

of the cell. Here, we see no different between the WT and KO -derived glands indicating the proton pump is functioning, just like Nishi et al. [70] reported.

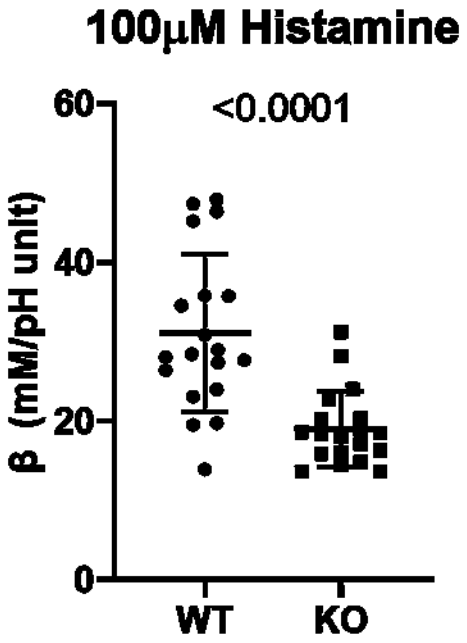

Figure 14 Cells from TRIM50 KO mice have reduced buffering power

β was calculated using Equations 1 and 2.

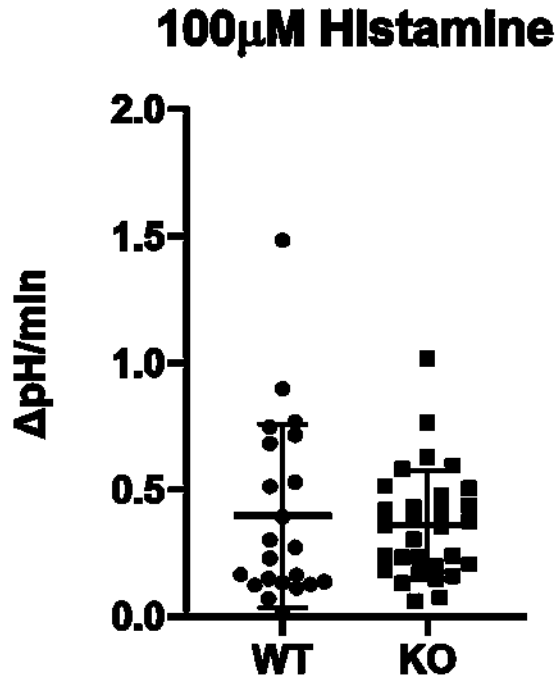

Figure 15 Deletion of TRIM50 does not alter ATP4A translocation or activity

The rate of acid secretion from the cell was calculated as the slope between pH_i 6.6-6.8 for all cells.

Discussion

Overall, the experiments presented here indicate TRIM50 may be involved in maintenance of intracellular pH buffering (Figures 10 and 13). Additionally, the majority of intracellular trafficking of TRIM50-associated vesicles appears to be through the molecular motor dynein on microtubules and not strongly on the actin cytoskeleton (Figure 15). When the minimal inhibition of TRIM50 associated vesicle movement is taken in conjunction with the fact there is no difference in the rate of acid secretion from the WT and KO cells (Figure 14), we believe this indicates it is not likely TRIM50 directly interacts with ATP4A vesicles to drive acid secretion.

When characterizing the role of TRIM50, Nishi et al. described an increase in multi-lamellated structures in the gastric parietal tissue of KO mice, leading to the conclusion that TRIM50 may be directly involved in intracellular vesicle trafficking of ATP4A-associated vesicles [70]. As noted by Nishi et al. the formation of multi-lamellar compartments appears to be a normal aspect of gastric acid secretion during the vesicle re-uptake phase of ATP4A-associated vesicles [70, 100]. The multi-lamellar vesicles formed as autophagosomes during the endocytotic pathway can then develop into Golgi apparatus and lysosomal compartments [100]. Recently, Fusco et al. has shown that TRIM50 directly interacts with p62/Sequestosome1 for clearance of polyubiquitinated proteins in the aggresome via its PRY/SPRY domain [80, 81]. TRIM50 also interacts with Beclin1, another protein essential to initiation of autophagy through the regulation of PI3K, to positively regulate the initiation phase of starvation-induced autophagy [82].

The pathology seen by Nishi et al. [70] may be related to TRIM50's regulation of autophagosome formation.

Similar pathologies to TRIM50 deletion-mediated dysregulation of pH and the formation of multi-lamellar membranes after secretion are seen in parietal cells from transient receptor potential mucolipin 1 (TRPML1) [101], AE2 (anion exchanger 2, Cl^-/HCO_3^- exchanger, *Slc4a2*) [102], or NHE2 (Na^+/H^+ exchanger 2, *Slc9a2*) [102] deficient mice. TRPML1 is an endo-lysosomal Ca^{2+} permeable channel, allowing both Ca^{2+} entry or release from lysosome and ER stores, whose deletion causes mucolipidosis type IV, a neurodegenerative lysosomal storage disorder, and chronic achlorhydria [101]. Interestingly, these exchangers all regulate intracellular pH, which is dysregulated in TRIM50 parietal cells (Figures 10, 12, and 13). This suggests TRIM50's E3 ubiquitin ligase function may actually be related to regulating intracellular pH buffering through mediation of aggresome/autophagosome formation or regulation of membranes associated with anion exchangers other than the ATP4A-associated acid transport function.

As mentioned before, TRIM50 is one of the 23 proteins deleted in Williams-Beuren syndrome [68]. RNA expression analysis of TRIM50 found on the Human Protein Atlas suggests it may be expressed in the liver, pancreas, and kidney as well as the stomach and testis [103]. Considering TRIM50 deletion results in aberrant intracellular homeostasis and secretion, TRIM50 deletion may be one of the causative factors of the hypercalcemia, digestive and urinary issues seen in Williams-Beuren

Syndrome patients. Further assessment of TRIM50 deletion in these other tissue types may help drive finding therapies to alleviate the symptoms of these unique patients.

Chapter 5: Role of PRY/SPRY Domain in Membrane Repair

Introduction

Although expressed in different tissues, TRIM50 and MG53 retain a high sequence homology as TRIM family proteins containing both an RBCC and a PRY/SPRY region and are categorized into the same subfamily of TRIM proteins [4, 5]. Between the two proteins, only the crystal structure for the MG53 PRY/SPRY domain has been solved [104]. From the crystal structure of MG53 and other TRIM proteins containing the PRY/SPRY domain, we know that there are 2 binding pockets formed by six variable loop domains which create specificity for each TRIM protein [16, 105]. Currently, we do not know what role the PRY/SPRY domains in MG53 and TRIM50 perform in relation to vesicle trafficking and wound healing and because we do not have an entire structure of MG53 or any part of TRIM50, all comparisons between the proteins must be done via mutagenic studies.

In 2009, Cai et al. identified cystine 242 as essential for oxidation-mediated oligomerization of MG53 [27]. Additionally, a leucine zipper motif in the coiled-coil domain of MG53 was shown to mediate intermolecular interaction and modulate the efficiency of the oxidation-mediated oligomerization [32]. Less is known about important TRIM50 domains. However Fusco et al. (2012) indicated the coiled-coil domain in the RBCC region of TRIM50 was needed for binding to p62, one of its interacting partners

[80]. Therefore, the goal of this project is to characterize functions of the MG53 PRY/SPRY domain through chimeric mutagenesis with TRIM50 and assessing for membrane repair function.

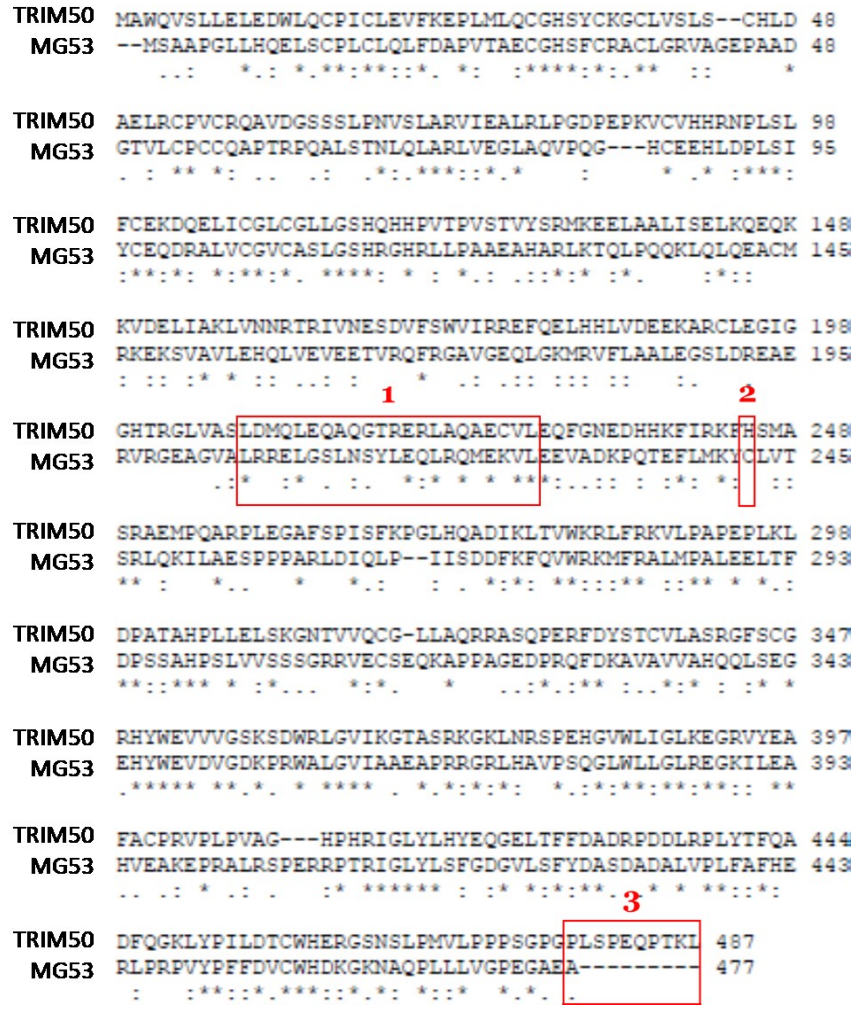

Figure 16 ClustalW alignment between TRIM50 and MG53

Box 1 shows the leucine zipper region in MG53, highlighting the missing leucine zipper region in TRIM50. Box 2 indicates MG53 cysteine 242 showing a histidine in the

corresponding TRIM50 location. Box 3 shows an extended tail on the TRIM50 SPRY domain.

Results

TRIM50 and MG53 have many amino acid sequences in common, however differ in several key areas, as indicated in Figure 16. In order to determine the PRY/SPRY function of MG53 in relation to subcellular localization, the GFP-TRIM50/MG53 mutant was expressed in HeLa cells and imaged under confocal microscopy. The chimera was generated with the TIM50 RBCC domain amino acids M1-I285 and the MG53 PRY/SPRY domain, including C242 with amino acids Q234-A477 and the sequence verified through sanger sequencing. Normally, MG53 localizes mainly at the plasma membrane and faintly throughout the cytoplasm, whereas TRIM50 typically forms punctae throughout the cytoplasm. Imaging of GFP-TRIM50/MG53 revealed a punctae-like pattern, similar to that seen with TRIM50 (Figure 17). This suggests there may be some domain on the N-terminal of TRIM50 and MG53 that drive their subcellular localization.

Because MG53 needs to sense changes in oxidative state in the cell to perform its membrane repair function, TRIM50/MG53 chimera's response to changes in oxidative state were assessed. HeLa cells transfected with mCherry-TRIM50, GFP-MG53 C242A, GFP-MG53, or GFP-TRIM50/MG53 were lysed in cold, non-reducing RIPA (50mM Tris-HCl, pH 7.4, 150mM NaCl, 1mM EDTA, 1% NP-40, and 1x protease inhibitor complex). Equal concentrations of lysates were diluted in 2x non-reducing SDS Loading

Buffer (125mM Tris-HCl pH 6.8, 4% SDS, 20% Glycerol, and 0.004% Bromophenol Blue) with increasing concentrations of DTT (0, 1, 10, 100mM) to de-oligomerize proteins. Figure 18 shows the TRIM50/MG53 chimera does oligomerize in an oxidative fashion and respond to changes in oxidative state, similar to MG53. TRIM50 and MG53 mutant C242A do not respond to changes in oxidative state. The oligomerization of the mutant still may be related to cysteine 242 as that was designed to be a part of the MG53 c-terminal domain in the chimera.

Finally, to determine whether the c-terminal domain is sufficient to convey membrane repair function to a TRIM RBCC domain, we performed 2 forms of mechanical injury to HeLa cells transfected with TRIM50/MG53. Figure 19A shows the chimera does not translocate to the plasma membrane and, in fact, the cell begins shrinking in size as in the beginning stages of apoptosis. We also performed an LDH release assay to gain a quantitative view of whether the TRIM50/MG53 chimera can participate in maintaining cell integrity. Figure 19B shows that, although MG53 prevents LDH release, as seen in previous publications, TRIM50 and the TRIM50/MG53 chimera do no prevent LDH release, indicating a lack of plasma membrane integrity.

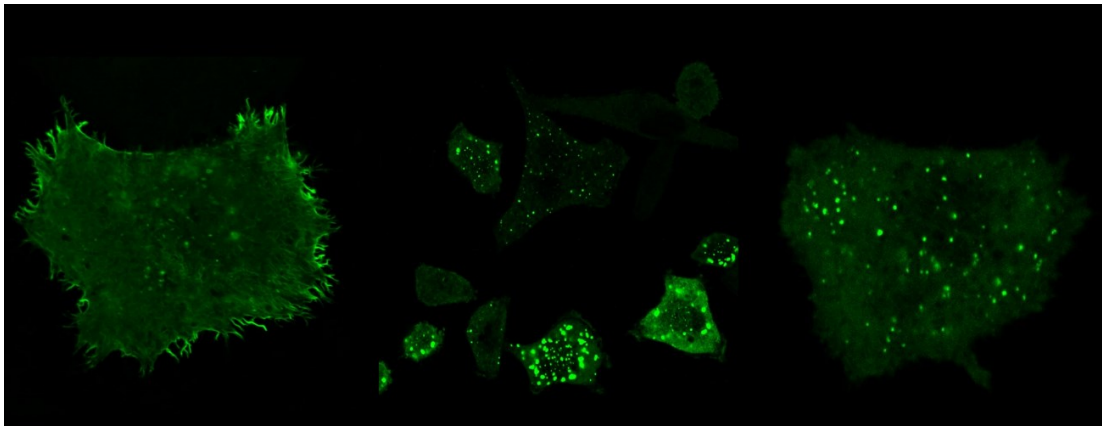

Figure 17 Localization of TRIM constructs

Hela cells were transfected with either GFP-MG53, mCherry-TRIM50, or GFP-TRIM50 RBCC domain/MG53 PRY/SPRY domain chimera and imaged on a confocal microscope for intracellular localization

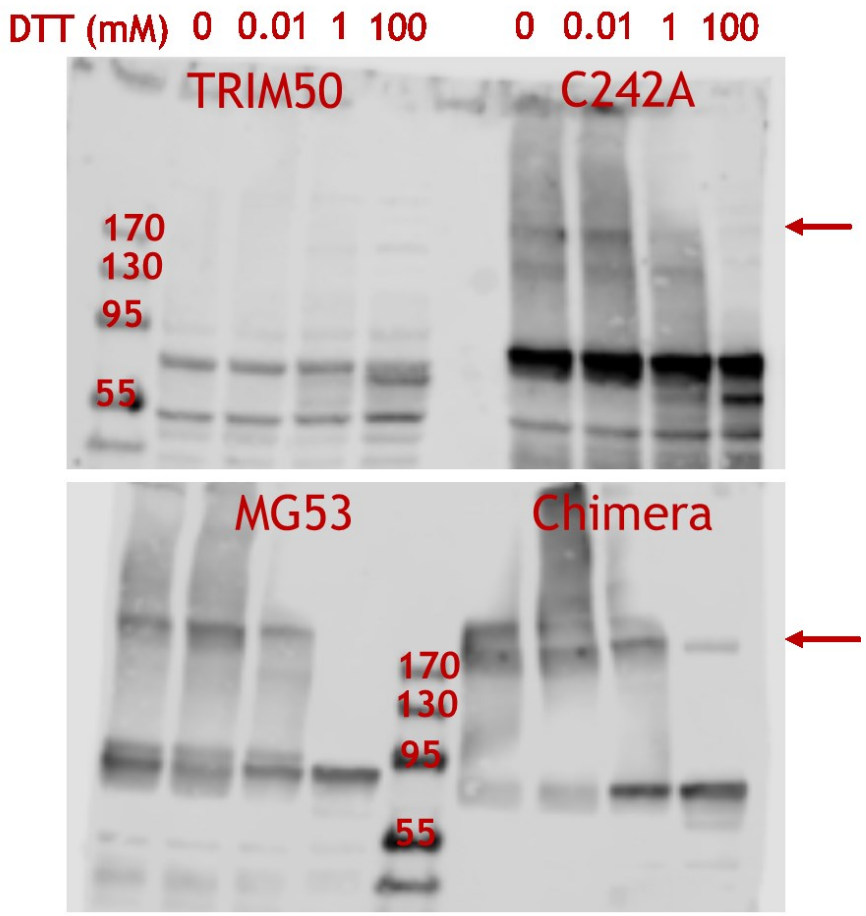

Figure 18 TRIM50/MG53 chimera dimerizes in oxidative conditions

Representative western blots of HeLa cells transfected with mCherry-TRIM50, GFP-MG53-C242A, GFP-MG53,or GFP-TRIM50/MG53 and subjected to increasing concentrations of DTT (0-100mM).

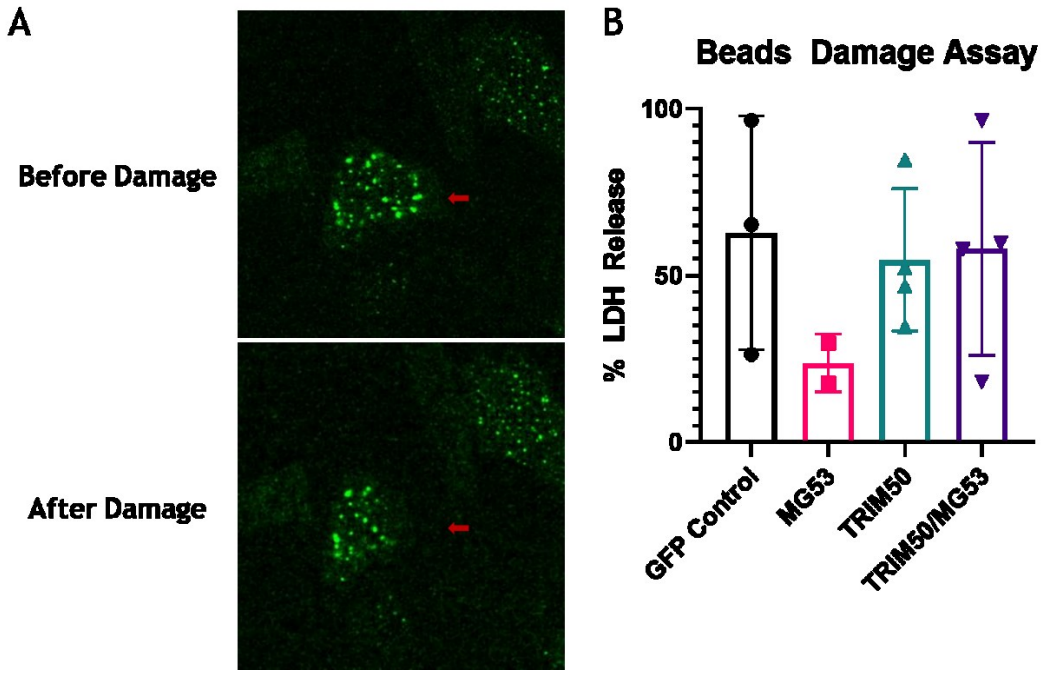

Figure 19 TRIM50/MG53 does not participate in plasma membrane repair

(A) HeLa cells transfected with GFP-TRIM50/MG53 were damaged with a microcapillary needle and monitored for 5 minutes. Red arrow indicates location of microcapillary needle injury. (B) % lactose dehydrogenase (LDH) release from beads damage assay of HeLa cells transfected with control GFP-C1, GFP-MG53, mCherry-TRIM50, or GFP-TRIM50/MG53

Discussion

Overall, this project indicates that the RBCC domain of MG53 necessary for cell membrane repair function and subcellular localization, as the chimera did not translocate to the injured plasma membrane or prevent LDH release after injury from microbeads damage (Figure 19). The MG53 PRY/SPRY domain is enough to cause a change in oligomerization in response to changes in oxidative state (Figure 18), however this was already established by Cai et al.[27] as being driven by cysteine 242 (C242), which is present in this construct. It is likely a construct that begins after C242 will not be capable of dimerization, similar to TRIM50.

One of the ways MG53 localizes to breaks in the plasma membrane and most likely localizes to the mitochondria is through preferential binding to phosphatidylserine and cardiolipin. The subcellular localization of the chimeric protein resembles that of TRIM50. This suggests the lipid binding domain of these proteins may be on the RBCC region, associated with one or a few amino acids the two proteins do not share, such as in the leucine zipper domain (Figure 16, Box 1) or around TRIM50 aa. 79-89 / MG53 aa. 79-87, an unusually divergent section of the RBCC region.

Currently, a mechanism for MG53 packaging into exosomes has not been determined. Because we have not seen any evidence of TRIM50 also being secreted into the blood, We suspect the packaging and secretion of MG53 is driven by the divergent PRY/SPRY domain. Assessing the ability of the chimera to be secreted from the cells will be another useful avenue of research in determining how MG53 is secreted as a myokine for tissue regeneration. Being able to implant stem cells with a modified MG53

protein for enhanced secretion into the bloodstream would be an extremely beneficial tool in the field of regenerative medicine. Therefore, determining the function of the PRY/SPRY domain of MG53 or elucidating the domain responsible for MG53 exosome packaging will be essential for future MG53 therapy research.

Chapter 6: Conclusions and Future Directions

Research on TRIM family proteins have been gaining notoriety, particularly for their functions in the innate immunity, oncogenesis, autophagy, and membrane repair. To this end, this work's goal is to build upon our current knowledge of TRIM family proteins by focusing on TRIM72 (MG53) and TRIM50.

In accordance with previously published literature, MG55 preserves cell function after ischemic injury, however evidence presented here provides a novel mechanism for that preservation by regulating mitophagy. By promoting mitophagy, MG53 effectively reduces mitochondrial ROS production while maintaining a healthy supply of ATP. Although this project focused on preserving myocardial function through the maintenance of cardiomyocytes the application of this novel function provides another basis for explaining how application of MG53 can restore injured cells and tissue function after major injuries like myocardial infarctions [39, 41], acute kidney injury [40], acute lung injury [44], and stroke [43]. Given the number of aging related diseases that result from ischemic injury or a buildup of damaged mitochondria, it is tempting to speculate the addition of MG53 as a therapy as we age may prevent the onset of disorders like Alzheimer's or Parkinson's disease. Indeed, a recently published study demonstrated MG53 can pass the blood brain barrier to heal injured neurons after traumatic brain injury [43]. Studies on MG53's mitochondria protection should focus on whether MG53

treatment can prevent or at least slow the progression of Parkinson's disease, which is often characterized neuronal loss in the substantia nigra, causing a reducing in dopamine production [106]. Treatment with exogenous MG53 may prevent loss of these neurons through the maintenance of a healthy mitochondrial population.

A limitation of this study as it stands is there is no direct readout of mitophagy. Rather mitophagy is inferred based on the prevention of ROS release (Figure 8) and increased mitochondrial fission (Figure 9). Current and future work on this project involve utilizing the innovative molecular tool, mt-Keima, to directly assess the rate of mitophagy in cells with rhMG53 treatment after oxidative stress [107, 108]. Additionally, a direct measurement of O_2 consumption and ATP production after oxidative damage and MG53 treatment will be required to prove MG53's preservation of mitochondria function. Future studies should also focus on whether MG53 can ubiquitinate proteins that are translocated to the outer mitochondrial membrane after oxidative injury. It is possible that MG53 may be involved in trafficking lipid rafts to the mitochondria to seal the mitochondrial permeability transition pore, the site of mitochondrial ROS release after mitochondrial damage. However, the mechanism for the increased fission seen in MG53-treated cells after oxidative damaged (Figure 9) must be assessed either way.

A second goal of this dissertation was to clarify the role of TRIM50 in gastric acid secretion. In conjunction with papers published by Fusco et al. [68, 80–82], the evidence provided in this work help clarify the role of TRIM50, particularly in relation to gastric acid secretion. Here, the data indicate TRIM50 is involved in mediating intracellular pH buffering (Figures 10, 12, and 13). Future studies on TRIM50 in

mediating intracellular buffering should assess whether TRIM50 is involved in Alkaline Flux, the balance of CO2 and bicarbonate into and out of the cell for intracellular pH buffering. Determining whether TRIM50 mediates the creation of protons from carbonic acid or the exchange between chloride and bicarbonate will be an essential next step in this project.

Other recent work on TRIM50 have implicated it in inhibiting oncogenesis in hepatocarcinoma [109] and possibly renal cancer (Figure 19) [110]. The paper by Xiaoxiao Ma et al. describes TRIM50's inhibition of hepatocarcinoma through K-48 polyubiquitination of SNAIL, a transcription factor that mediates the epithelial-to-mesenchymal transition (EMT) [109]. This function of TRIM50 is intriguing as some unpublished in the Ma lab suggests MG53 may also mediate the EMT process. TRIM50 acting as a cancer inhibiting factor may also explain how higher expression of TRIM50 is correlated with a longer survival probability of patients with renal cancer, as shown in Figure 19.

Some preliminary data in our lab (shown in Figure 20) indicates some TRIM50 KO mice spontaneously exhibit an elevated urine protein to creatinine ratio when compared to WT mice. The increase in urine protein to creatinine may signify kidney damage and/or chronic kidney disease. Because kidneys are responsible for systemic HCO_3^- concentration, dysregulation of intracellular pH buffering in renal cells may be responsible for the spontaneous development of proteinuria in TIRM50 KO mice. Some people affected by Williams-Beuren syndrome have reported digestive and urinary problems associated with hypoplasia and malformation of these organs. Studies

determining whether the deletion of TRIM50 is associated with the hypoplasia and malformation in relation to dysregulated intracellular pH buffering and lysosome formation in the cells.

A final goal of this project was to further characterize the role of MG53's PRY/SPRY domain in cell membrane repair through the generation of a TRIM chimera using the TRIM50 RBCC domain. Although the PRY/SPRY domain of MG53 was not sufficient to provide membrane repair functionality, future studies on whether the TRIM50/MG53 chimera may localize with mitochondria after oxidative stress injury would provide useful information on the newly described function of MG53. The generation of an MG53 RBCC TRIM50 PRY/SPRY chimera together with the current TRIM50/MG53 chimera will allow us to test for preferential lipid binding domains which appear to drive MG53 localization within the cell.

This dissertation describes a novel mechanism for MG53 as a mediator of mitochondrial protection after ischemic injury. Addition of extracellular MG53 was effective in preventing ROS-induced ROS-release from the mitochondria as well as promoting mitochondrial fission, an essential step in the mitophagy process. In addition to a novel role for MG53, this work updates the role of TRIM50's role in gastric acid secretion, showing how TRIM50 mediates intracellular pH balance . We propose this balance is associated with its previously described function in formation of the aggresome for p62/LC3-assocated lysosomal degradation of proteins and organelles. Finally, this dissertation clarifies that the PRY/SPRY domain is not sufficient for driving plasma membrane repair, even with the ability for oxidation-associated oligomerization,

an essential component for MG53 membrane repair. The three projects presented herein adds to our understanding of TRIM family proteins and their role in health and disease while driving new directions for future TRIM research.

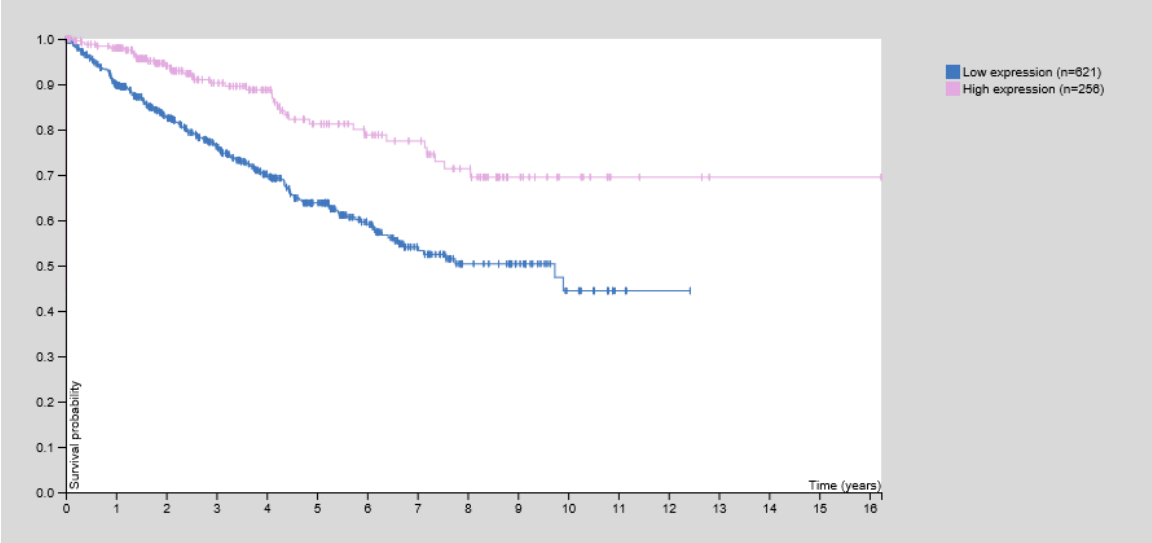

Figure 20 TRIM50 expression may be predictive of renal cancer outcomes

Kaplan-Meier curve of renal cancer patients with low (blue) and high (pink) TRIM50 expression from the Human Protein Atlas [110] available from https://www.proteinatlas.org/ENSG00000146755-TRIM50/pathology/tissue/renal+cancer

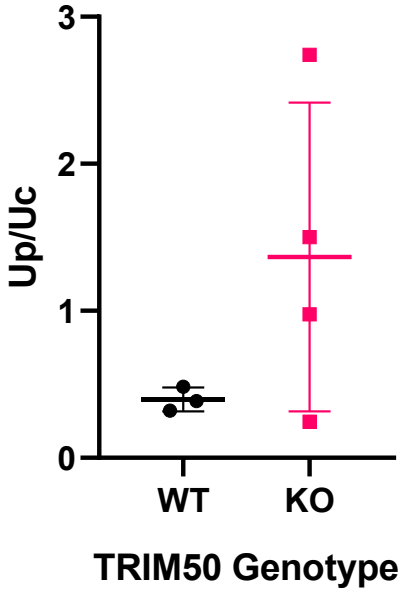

Figure 21 TRIM50 KO mice may develop proteinuria

Urine from TRIM50 WT and KO mice was collected for 12 hours in a metabolic cage and assayed for protein and creatinine content.

List of Cited References

1. Neefjes J, Groothuis TAM, Dantuma NP (2004) The 2004 Nobel Prize in Chemistry for the discovery of ubiquitin-mediated protein degradation. Ned Tijdschr Geneeskd 148:2579–82
2. Lee I, Schindelin H (2008) Structural Insights into E1-Catalyzed Ubiquitin Activation and Transfer to Conjugating Enzymes. Cell 134:268–278
3. Zheng N, Shabek N (2017) Ubiquitin Ligases: Structure, Function, and Regulation. Annu Rev Biochem 86:129–157
4. Ozato K, Shin D-M, Chang T-H, Morse HC, III (2008) TRIM family proteins and their emerging roles in innate immunity. Nat Rev Immunol 8:849–60
5. Hatakeyama S (2017) TRIM Family Proteins: Roles in Autophagy, Immunity, and Carcinogenesis. Trends Biochem Sci 42:297–311
6. Lee H-J (2018) The Role of Tripartite Motif Family Proteins in TGF-β Signaling Pathway and Cancer. J cancer Prev 23:162–169
7. Mandell MA, Jain A, Arko-Mensah J, et al (2014) TRIM proteins regulate autophagy and can target autophagic substrates by direct recognition. Dev Cell 30:394
8. Sardiello M, Cairo S, Fontanella B, Ballabio A, Meroni G (2008) Genomic analysis of the TRIM family reveals two groups of genes with distinct evolutionary properties. BMC Evol Biol 8:225
9. Herquel B, Ouararhni K, Davidson I (2011) The TIF1α-related TRIM cofactors couple chromatin modifications to transcriptional regulation, signaling and tumor suppression. Transcription 2:231–6
10. Ragvin A, Valvatne H, Erdal S, et al (2004) Nucleosome Binding by the Bromodomain and PHD Finger of the Transcriptional Cofactor p300. J Mol Biol 337:773–788
11. Stevens R V, Esposito D, Rittinger K (2019) Characterisation of class VI TRIM RING domains: linking RING activity to C-terminal domain identity. Life Sci alliance 2:e201900295
12. Witt SH, Granzier H, Witt CC, Labeit S (2005) MURF-1 and MURF-2 Target a Specific Subset of Myofibrillar Proteins Redundantly: Towards Understanding MURF-dependent Muscle Ubiquitination. J Mol Biol 350:713–722
13. Lodka D, Pahuja A, Geers-Knörr C, et al (2016) Muscle RING-finger 2 and 3 maintain striated-muscle structure and function. J Cachexia Sarcopenia Muscle 7:165–80
14. Wang G, Biswas AK, Ma W, et al (2018) Metastatic cancers promote cachexia through ZIP14 upregulation in skeletal muscle. Nat Med 24:770–781
15. LECKER SH, JAGOE RT, GILBERT A, GOMES M, BARACOS V, BAILEY J,

PRICE SR, MITCH WE, GOLDBERG AL (2004) Multiple types of skeletal muscle atrophy involve a common program of changes in gene expression. FASEB J 18:39–51
16. James LC, Keeble AH, Khan Z, Rhodes DA, Trowsdale J (2007) Structural basis for PRYSPRY-mediated tripartite motif (TRIM) protein function. Proc Natl Acad Sci U S A 104:6200–5
17. D'Cruz AA, Babon JJ, Norton RS, Nicola NA, Nicholson SE (2013) Structure and function of the SPRY/B30.2 domain proteins involved in innate immunity. Protein Sci 22:1
18. Sebastian S, Luban J (2005) TRIM5alpha selectively binds a restriction-sensitive retroviral capsid. Retrovirology 2:40
19. Zhao J, Lei H (2016) Tripartite Motif Protein 72 Regulates the Proliferation and Migration of Rat Cardiac Fibroblasts via the Transforming Growth Factor-β Signaling Pathway. Cardiology 134:340–346
20. Li H, Duann P, Lin P-H, et al (2015) Modulation of Wound Healing and Scar Formation by MG53 Protein-mediated Cell Membrane Repair. J Biol Chem 290:24592–24603
21. Harr MW, Distelhorst CW (2010) Apoptosis and autophagy: decoding calcium signals that mediate life or death. Cold Spring Harb Perspect Biol 2:a005579
22. Moe A, Golding AE, Bement WM (2015) Cell healing: calcium, repair and regeneration. Semin Cell Dev Biol 45:18
23. Xu T, Naraghi M, Kang H, Neher E (1997) Kinetic studies of Ca2+ binding and Ca2+ clearance in the cytosol of adrenal chromaffin cells. Biophys J 73:532–545
24. Cheng X, Zhang X, Yu L, Xu H (2015) Calcium signaling in membrane repair. Semin Cell Dev Biol 45:24–31
25. McNeil PL, Vogel SS, Miyake K, Terasaki M (2000) Patching plasma membrane disruption with cytoplasmic membrane. J Cell Sci 113:1891–1902
26. Bouter A, Gounou C, Bérat R, Tan S, Gallois B, Granier T, d'Estaintot BL, Pöschl E, Brachvogel B, Brisson AR (2011) Annexin-A5 assembled into two-dimensional arrays promotes cell membrane repair. Nat Commun 2:270
27. Cai C, Masumiya H, Weisleder N, et al (2009) MG53 nucleates assembly of cell membrane repair machinery. Nat Cell Biol 11:56–64
28. Cai C, Weisleder N, Ko J-K, Komazaki S, Sunada Y, Nishi M, Takeshima H, Ma J (2009) Membrane Repair Defects in Muscular Dystrophy Are Linked to Altered Interaction between MG53, Caveolin-3, and Dysferlin. J Biol Chem 284:15894–15902
29. Weisleder N, Takizawa N, Lin P, et al (2012) Recombinant MG53 protein modulates therapeutic cell membrane repair in treatment of muscular dystrophy. Sci Transl Med 4:139ra85
30. Wang C, Vernon R, Lange O, Tyka M, Baker D (2010) Prediction of structures of zinc-binding proteins through explicit modeling of metal coordination geometry. Protein Sci 19:NA-NA
31. Lin P, Zhu H, Cai C, Wang X, Cao C, Xiao R, Pan Z, Weisleder N, Takeshima H, Ma J (2012) Nonmuscle myosin IIA facilitates vesicle trafficking for MG53-

mediated cell membrane repair. FASEB J 26:1875–83
32. Hwang M, Ko J-K, Weisleder N, Takeshima H, Ma J (2011) Redox-dependent oligomerization through a leucine zipper motif is essential for MG53-mediated cell membrane repair. Am J Physiol Cell Physiol 301:C106-14
33. Cai C, Lin P, Zhu H, Ko J-K, Hwang M, Tan T, Pan Z, Korichneva I, Ma J (2015) Zinc Binding to MG53 Protein Facilitates Repair of Injury to Cell Membranes. J Biol Chem 290:13830–9
34. Gumpper K, Ma J (2019) Zinc Signaling in Skeletal Muscle. Zinc Signals Cell. Funct. Disord.
35. He B, Tang R, Weisleder N, et al (2012) Enhancing Muscle Membrane Repair by Gene Delivery of MG53 Ameliorates Muscular Dystrophy and Heart Failure in δ-Sarcoglycan-deficient Hamsters. Mol Ther 20:727–735
36. Weisleder N, Takizawa N, Lin P, et al (2012) Recombinant MG53 protein modulates therapeutic cell membrane repair in treatment of muscular dystrophy. Sci Transl Med 4:139ra85
37. Alloush J, Weisleder N (2013) TRIM proteins in therapeutic membrane repair of muscular dystrophy. JAMA Neurol 70:928–31
38. Ayodele Adesanya TM, Russell M, Park KH, et al (2019) MG53 protein protects aortic valve interstitial cells from membrane injury and Fibrocalcific Remodeling. J Am Heart Assoc. doi: 10.1161/JAHA.118.009960
39. Wang X, Xie W, Zhang Y, et al (2010) Cardioprotection of Ischemia/Reperfusion Injury by Cholesterol-Dependent MG53-Mediated Membrane Repair. Circ Res 107:76–83
40. Duann P, Li H, Lin P, et al (2015) MG53-mediated cell membrane repair protects against acute kidney injury. Sci Transl Med 7:279ra36
41. Liu J, Zhu H, Zheng Y, et al (2015) Cardioprotection of recombinant human MG53 protein in a porcine model of ischemia and reperfusion injury. J Mol Cell Cardiol 80:10–19
42. Zhu H, Hou J, Roe JL, et al (2015) Amelioration of ischemia-reperfusion-induced muscle injury by the recombinant human MG53 protein. Muscle Nerve 52:852–858
43. Yao Y, Zhang B, Zhu H, et al (2016) MG53 permeates through blood-brain barrier to protect ischemic brain injury. Oncotarget 7:22474–85
44. Jia Y, Chen K, Lin P, et al (2014) Treatment of acute lung injury by targeting MG53-mediated cell membrane repair. Nat Commun 5:4387
45. Cao C-M, Zhang Y, Weisleder N, et al (2010) MG53 Constitutes a Primary Determinant of Cardiac Ischemic Preconditioning. Circulation 121:2565–2574
46. Gushchina L V, Bhattacharya S, McElhanon KE, Choi JH, Manring H, Beck EX, Alloush J, Weisleder N (2017) Treatment with Recombinant Human MG53 Protein Increases Membrane Integrity in a Mouse Model of Limb Girdle Muscular Dystrophy 2B. Mol Ther 25:2360–2371
47. Nguyen N, Yi J-S, Park H, Lee J-S, Ko Y-G (2014) Mitsugumin 53 (MG53) ligase ubiquitinates focal adhesion kinase during skeletal myogenesis. J Biol Chem 289:3209–16

48. Graham ZA, Gallagher PM, Cardozo CP (2015) Focal adhesion kinase and its role in skeletal muscle. J Muscle Res Cell Motil 36:305–15
49. Ma H, Liu J, Bian Z, et al (2015) Effect of Metabolic Syndrome on Mitsugumin 53 Expression and Function. PLoS One 10:e0124128
50. Hu X, Xiao R-P (2018) MG53 and disordered metabolism in striated muscle. Biochim Biophys Acta - Mol Basis Dis 1864:1984–1990
51. Song R, Peng W, Zhang Y, et al (2013) Central role of E3 ubiquitin ligase MG53 in insulin resistance and metabolic disorders. Nature 494:375–379
52. Yi J-S, Park JS, Ham Y-M, et al (2013) MG53-induced IRS-1 ubiquitination negatively regulates skeletal myogenesis and insulin signalling. Nat Commun 4:2354
53. Liu F, Song R, Feng Y, et al (2015) Upregulation of MG53 Induces Diabetic Cardiomyopathy Through Transcriptional Activation of Peroxisome Proliferation-Activated Receptor α. Circulation 131:795–804
54. Qi J, Yang B, Ren C, Fu J, Zhang J (2016) Swimming Exercise Alleviated Insulin Resistance by Regulating Tripartite Motif Family Protein 72 Expression and AKT Signal Pathway in Sprague-Dawley Rats Fed with High-Fat Diet. J Diabetes Res 2016:1564386
55. Tamemoto H, Kadowaki T, Tobe K, et al (1994) Insulin resistance and growth retardation in mice lacking insulin receptor substrate-1. Nature 372:182–186
56. Laustsen PG, Michael MD, Crute BE, Cohen SE, Ueki K, Kulkarni RN, Keller SR, Lienhard GE, Kahn CR (2002) Lipoatrophic diabetes in Irs1(-/-)/Irs3(-/-) double knockout mice. Genes Dev 16:3213–22
57. Harman D (1956) Aging: A Theory Based on Free Radical and Radiation Chemistry. J Gerontol 11:298–300
58. Kadenbach B, Ramzan R, Vogt S (2009) Degenerative diseases, oxidative stress and cytochrome c oxidase function. Trends Mol Med 15:139–147
59. Flynn JM, Melov S (2013) SOD2 in mitochondrial dysfunction and neurodegeneration. Free Radic Biol Med 62:4–12
60. Zorov DB, Juhaszova M, Sollott SJ (2014) Mitochondrial reactive oxygen species (ROS) and ROS-induced ROS release. Physiol Rev 94:909–50
61. Zorov DB, Filburn CR, Klotz LO, Zweier JL, Sollott SJ (2000) Reactive oxygen species (ROS)-induced ROS release: a new phenomenon accompanying induction of the mitochondrial permeability transition in cardiac myocytes. J Exp Med 192:1001–14
62. Rana A, Oliveira MP, Khamoui A V., Aparicio R, Rera M, Rossiter HB, Walker DW (2017) Promoting Drp1-mediated mitochondrial fission in midlife prolongs healthy lifespan of Drosophila melanogaster. Nat Commun 8:448
63. Narendra DP, Jin SM, Tanaka A, Suen D-F, Gautier CA, Shen J, Cookson MR, Youle RJ (2010) PINK1 is selectively stabilized on impaired mitochondria to activate Parkin. PLoS Biol 8:e1000298
64. Ding W-X, Yin X-M (2012) Mitophagy: mechanisms, pathophysiological roles, and analysis. Biol Chem 393:547–64
65. Lazarou M, Sliter DA, Kane LA, Sarraf SA, Wang C, Burman JL, Sideris DP,

Fogel AI, Youle RJ (2015) The ubiquitin kinase PINK1 recruits autophagy receptors to induce mitophagy. Nature 524:309–314
66. McWilliams TG, Prescott AR, Montava-Garriga L, Ball G, Singh F, Barini E, Muqit MMK, Brooks SP, Ganley IG (2018) Basal Mitophagy Occurs Independently of PINK1 in Mouse Tissues of High Metabolic Demand. Cell Metab 27:439-449.e5
67. Huang ML-H, Chiang S, Kalinowski DS, Bae D-H, Sahni S, Richardson DR (2019) The Role of the Antioxidant Response in Mitochondrial Dysfunction in Degenerative Diseases: Cross-Talk between Antioxidant Defense, Autophagy, and Apoptosis. Oxid Med Cell Longev 2019:1–26
68. Micale L, Fusco C, Augello B, Napolitano LMR, Dermitzakis ET, Meroni G, Merla G, Reymond A (2008) Williams–Beuren syndrome TRIM50 encodes an E3 ubiquitin ligase. Eur J Hum Genet 16:1038–1049
69. Pober BR (2010) Williams–Beuren Syndrome. N Engl J Med 362:239–252
70. Nishi M, Aoyama F, Kisa F, et al (2012) TRIM50 Protein Regulates Vesicular Trafficking for Acid Secretion in Gastric Parietal Cells. J Biol Chem 287:33523–33532
71. Betesh AL, Santa Ana CA, Cole JA, Fordtran JS (2015) Is achlorhydria a cause of iron deficiency anemia? Am J Clin Nutr 102:9–19
72. Tavares M, Dias JA (2017) Long-Term Effects of Achlorhydria on the Stomach (Helicobacter pylori and PPI Therapy). In: Esophageal Gastric Disord. Infancy Child. Springer Berlin Heidelberg, Berlin, Heidelberg, pp 1387–1395
73. Lin Y-S, Huang T-T, Hsu Y-J, Lin JY-T, Wu C-H, Hu Y-H (2015) Refractory hypocalcemia and hypomagnesemia associated with the use of an oral proton-pump inhibitor in a patient with hypoparathyroidism. Tzu Chi Med J 27:175–176
74. Kinoshita Y, Ishimura N, Ishihara S (2018) Advantages and Disadvantages of Long-term Proton Pump Inhibitor Use. J Neurogastroenterol Motil 24:182–196
75. Nehra AK, Alexander JA, Loftus CG, Nehra V (2018) Proton Pump Inhibitors: Review of Emerging Concerns. Mayo Clin Proc 93:240–246
76. Kheloussi S (2017) Appropriate Use and Safety Concerns of Proton Pump Inhibitors. US Pharm 42:38–42
77. Sanchis-Gomar F, Perez-Quilis C, Leischik R, Lucia A (2016) Epidemiology of coronary heart disease and acute coronary syndrome. Ann Transl Med. doi: 10.21037/ATM.2016.06.33
78. Mozaffarian D, Benjamin EJ, Go AS, et al (2015) Heart Disease and Stroke Statistics—2015 Update. Circulation. doi: 10.1161/CIR.0000000000000152
79. Maxwell S (1999) Emergency management of acute myocardial infarction. Br J Clin Pharmacol 48:284–98
80. Fusco C, Micale L, Egorov M, et al (2012) The E3-ubiquitin ligase TRIM50 interacts with HDAC6 and p62, and promotes the sequestration and clearance of ubiquitinated proteins into the aggresome. PLoS One 7:e40440
81. Fusco C, Micale L, Augello B, et al (2014) HDAC6 mediates the acetylation of TRIM50. Cell Signal 26:363–369
82. Fusco C, Mandriani B, Di Rienzo M, et al (2018) TRIM50 regulates Beclin 1

proautophagic activity. Biochim Biophys Acta - Mol Cell Res 1865:908–919
83. Sun M, Huang J, Bunyak F, Gumpper K, De G, Sermersheim M, Liu G, Lin P-H, Palaniappan K, Ma J (2014) Superresolution microscope image reconstruction by spatiotemporal object decomposition and association: Application in resolving t-tubule structure in skeletal muscle. Opt Express. doi: 10.1364/OE.22.012160
84. Huang J, Gumpper K, Chi Y, Sun M, Ma J (2015) Fast two-dimensional super-resolution image reconstruction algorithm for ultra-high emitter density. Opt Lett. doi: 10.1364/OL.40.002989
85. Gliddon BL, Nguyen N V, Gunn PA, Gleeson PA, van Driel IR (2008) Isolation, culture and adenoviral transduction of parietal cells from mouse gastric mucosa. Biomed Mater 3:034117
86. Engelstoft MS, Park W, Sakata I, et al (2013) Seven transmembrane G protein-coupled receptor repertoire of gastric ghrelin cells. Mol Metab 2:376–392
87. Sahoo N, Gu M, Zhang X, et al (2017) Gastric Acid Secretion from Parietal Cells Is Mediated by a Ca2+ Efflux Channel in the Tubulovesicle. Dev Cell 41:262-273.e6
88. Webster KA (2012) Mitochondrial membrane permeabilization and cell death during myocardial infarction: roles of calcium and reactive oxygen species. Future Cardiol 8:863–84
89. Yao W, Li H, Han X, Chen C, Zhang Y, Tai WL, Xia Z, Hei Z (2017) MG53 anchored by dysferlin to cell membrane reduces hepatocyte apoptosis which induced by ischaemia/reperfusion injury in vivo and in vitro. J Cell Mol Med 21:2503–2513
90. Lijie G, Yueyue Z, Nan Z, Ling W, Xuan W, Weijie Y (2019) Mitsugumin 53 promotes mitochondrial autophagy through regulating Ambra1 expression in C2C12 myoblast cells. Cell Biol Int 43:290–298
91. Åström-Olsson K, Li L, Olofsson CS, Borén J, Öhlin H, Grip L (2012) Impact of hypoxia, simulated ischemia and reperfusion in HL-1 cells on the expression of FKBP12/FKBP12.6 and intracellular calcium dynamics. Biochem Biophys Res Commun 422:732–738
92. Chu CT, Ji J, Dagda RK, et al (2013) Cardiolipin externalization to the outer mitochondrial membrane acts as an elimination signal for mitophagy in neuronal cells. Nat Cell Biol 15:1197–1205
93. Ryan T, Bamm V V., Stykel MG, et al (2018) Cardiolipin exposure on the outer mitochondrial membrane modulates α-synuclein. Nat Commun 9:817
94. Strappazzon F, Cecconi F (2015) AMBRA1-induced mitophagy: A new mechanism to cope with cancer? Mol Cell Oncol 2:e975647
95. Lemckert FA, Bournazos A, Eckert DM, et al (2016) Lack of MG53 in human heart precludes utility as a biomarker of myocardial injury or endogenous cardioprotective factor. Cardiovasc Res 110:178–187
96. Wu H-K, Zhang Y, Cao C-M, et al (2019) Glucose-Sensitive Myokine/Cardiokine MG53 Regulates Systemic Insulin Response and Metabolic Homeostasis. Circulation 139:901–914
97. Bian Z, Wang Q, Zhou X, et al (2019) Sustained Elevation of MG53 in the

Bloodstream Increases Tissue Regenerative Capacity without Compromising Metabolic Function. Nat Commun In press
98. Ito H, Oda N, Ito M, Kameda T, Nakayama H, Tahara E (1989) Cytogenetical Analysis of the Human Gastric Carcinoma Cell Line TMK-1.
99. Rotte A, Pasham V, Bhandaru M, et al (2010) Regulation of Gastric Acid Secretion by PKB/Akt2. Cell Physiol Biochem 25:695
100. Sawaguchi A, Aoyama F, Ohashi M, Ide S, Suganuma T (2006) Ultrastructural transformation of gastric parietal cells reverting from the active to the resting state of acid secretion revealed in isolated rat gastric mucosa model processed by high-pressure freezing. J Electron Microsc (Tokyo) 55:97–105
101. Kilpatrick BS, Yates E, Grimm C, Schapira AH, Patel S (2016) Endo-lysosomal TRP mucolipin-1 channels trigger global ER Ca2+ release and Ca2+ influx. J Cell Sci 129:3859–3867
102. Miller ML, Andringa A, Zavros Y, Bradford EM, Shull GE (2010) Volume Density, Distribution, and Ultrastructure of Secretory and Basolateral Membranes and Mitochondria Predict Parietal Cell Secretory (Dys)function. J Biomed Biotechnol 2010:394198
103. Uhlen M, Fagerberg L, Hallstrom BM, et al (2015) Tissue-based map of the human proteome. Science (80-) 347:1260419–1260419
104. Park EY, Kwon O-B, Jeong B-C, Yi J-S, Lee CS, Ko Y-G, Song HK (2009) Crystal structure of PRY-SPRY domain of human TRIM72. Proteins Struct Funct Bioinforma 78:NA-NA
105. Grütter C, Briand C, Capitani G, Mittl PRE, Papin S, Tschopp J, Grütter MG (2006) Structure of the PRYSPRY-domain: Implications for autoinflammatory diseases. FEBS Lett 580:99–106
106. Poewe W, Seppi K, Tanner CM, Halliday GM, Brundin P, Volkmann J, Schrag A-E, Lang AE (2017) Parkinson disease. Nat Rev Dis Prim 3:17013
107. Katayama H, Kogure T, Mizushima N, Yoshimori T, Miyawaki A (2011) A Sensitive and Quantitative Technique for Detecting Autophagic Events Based on Lysosomal Delivery. Chem Biol 18:1042–1052
108. Sun N, Yun J, Liu J, et al (2015) Measuring In Vivo Mitophagy. Mol Cell 60:685–96
109. Ma X, Ma X, Qiu Y, et al (2018) TRIM50 suppressed hepatocarcinoma progression through directly targeting SNAIL for ubiquitous degradation. Cell Death Dis 9:608
110. Uhlen M, Zhang C, Lee S, et al (2017) A pathology atlas of the human cancer transcriptome. Science 357:eaan2507
111. Dolman NJ, Chambers KM, Mandavilli B, Batchelor RH, Janes MS (2013) Tools and techniques to measure mitophagy using fluorescence microscopy. Autophagy 9:1653–1662